forests

MDPI

Article

Response of Vegetation Coverage to Climate Changes in the Qinling-Daba Mountains of China

Han Ren, Chaonan Chen, Yanhong Li, Wenbo Zhu *, Lijuan Zhang, Liyuan Wang and Lianqi Zhu

College of Geography and Environment, Henan University, Kaifeng 475004, China
* Correspondence: zhuwb517@163.com

Abstract: As a major component of the north–south transition zone in China, the vegetation ecosystem of the Qinling-Daba Mountains (QBM) is highly sensitive to climate change. However, the impact of sunshine duration, specifically, on regional vegetation remains unclear. By using linear trend, correlation, and multiple regression analyses, this study systematically analyzed the spatiotemporal characteristics and trend changes of the vegetation coverage in the QBM from 2000–2020. Changes in the main climate elements in different periods and the responses to them are also discussed. Over the past 21 years, the vegetation coverage on the east and west sides of the QBM has been lower than that in the central areas. However, it is showing a continuously improving trend, especially in winters and springs. The findings indicate that change of *FVC* in the QBM exhibited a positive correlation with temperature, a negative correlation with sunshine hours, and both positive and negative correlation with precipitation. On an annual scale, average temperature was the main controlling climatic factor. On a seasonal scale, the area dominated by precipitation in spring was larger. In summer, the relative importance of the three was weak. In autumn and winter, sunshine duration became the main factor affecting vegetation coverage in most areas.

Keywords: the Qinling-Daba Mountains; vegetation coverage; climatic factors; main control factor

Citation: Ren, H.; Chen, C.; Li, Y.; Zhu, W.; Zhang, L.; Wang, L.; Zhu, L. Response of Vegetation Coverage to Climate Changes in the Qinling-Daba Mountains of China. *Forests* **2023**, *14*, 425. https://doi.org/10.3390/f14020425

Academic Editor: Romà Ogaya

Received: 17 January 2023
Revised: 10 February 2023
Accepted: 15 February 2023
Published: 19 February 2023

1. Introduction

Terrestrial ecosystems are the basis for human survival and sustainable development. As an important part of the terrestrial ecosystem, vegetation is a link among ecological elements such as soil, hydrology, and atmosphere, and plays an important role in improving regional microclimate, purifying air, containing water, maintaining soil and water, and in the process of ecosystem evolution [1]. Vegetation change is a concrete manifestation of the change of human living environment, and plays the role of "indicator" in the study of global or regional environmental change. Therefore, monitoring and attribution analysis of regional vegetation cover dynamics has become an important part of global change research.

Climate change has a major impact on the structure and function of global ecosystems [2]. Among the different climate factors, temperature and precipitation are generally considered to be the key factors affecting vegetation growth and development. Temperature is a regulator of vegetation growth, especially at high latitudes and high altitudes. In recent decades, increased vegetation activity in the Northern Hemisphere has been related to an increase in temperature [3–5]. This is because warmer temperatures extend the vegetation growing season and increase the efficiency of photosynthesis and water use for vegetation growth [6]. However, temperature can also have a negative impact on vegetation, as exceeding the temperature required for optimal vegetation growth can lead to inhibition of photosynthesis. At higher temperatures, nutrient consumption due to respiration increases, thus limiting the growth of vegetation [7]. Precipitation is another key climatic factor regulating vegetation growth, as it increases soil moisture, which is essential to promote plant root activity and the water status of the vegetation. Several

studies have shown that the correlation between vegetation change and precipitation in the Northern Hemisphere has increased in recent years [8,9]. In addition, some studies have confirmed that sunshine duration, relative humidity, and wind speed are also important factors affecting vegetation growth. For example, results showed that the annual sunshine hours in the Qilian Mountains had the greatest explanatory power for regional vegetation changes from 2000 to 2020 [10]. Throughout the Tibetan Plateau region, relative humidity and water vapor pressure play a dominant role in the variation of vegetation during the growing season [11].

Mountains are the most active interface and the most vulnerable geographical unit in terrestrial ecosystems and are the drivers and amplifiers of environmental change. Therefore, mountain vegetation ecosystems are more sensitive to global changes. The Qiling and Daba Mountains (QBM) constitute a complete geographical unit in the center of China's interior. Not only are they a main part of China's north–south transition zone, but they also provide an important ecological channel connecting China's eastern plains and the Qinghai Tibet Plateau. The special geographical location and complex landform conditions render the vegetation ecosystem in the QBM highly sensitive to climate change. Monitoring the dynamics of vegetation cover in the QBM and studying their relationship with climate elements are crucial for assessing the environmental quality of regional ecosystems and maintaining optimal ecosystem functions.

Research has covered the dynamic changes in vegetation [12,13] and its driving factors in some areas of the QBM [14–18]. These studies are valuable for understanding local vegetation-climate relationships in the QBM. However, current studies on the relationship between vegetation pattern evolution and climatic factors in the QBM mostly focus on two factors, temperature, and precipitation, ignoring the impact of sunshine duration on regional vegetation change, and the relationship between them is not clear. In addition, previous studies have usually used simple correlation analysis methods to investigate the response of vegetation change to changes in a single climatic factor, but rarely have multiple climatic elements been integrated to identify the main controlling climatic factors affecting regional vegetation cover change, ignoring the spatial variation characteristics of vegetation change response to climate change. Therefore, the purpose of the present study was to use MODIS-NDVI and meteorological station data of long time series to identify the characteristics of vegetation coverage distribution and spatiotemporal changes in the QBM from 2000–2020 and explore the response mechanism to climate factor changes. Specifically, the main contents of this study are as follows: (1) the spatiotemporal variation characteristics of vegetation coverage and main climate elements during 2000–2020; (2) the response mechanism of vegetation coverage change to a single climate factor; and (3) the main climate factor changes of regional vegetation coverage during different periods.

2. Data and Methods

2.1. Study Area

The QBM is in central China between 102 ° E–114 ° E and 30 ° N–36 ° N (Figure 1a). It stretches across Gansu, Sichuan, Shaanxi, Chongqing, Hubei, and Henan from west to east, with a total area of approximately 3.0 × 105 km^2. The altitude gradually rises from east to west. The QBM includes three major geomorphic units: Qinling Mountains, Daba Mountains and Hanjiang Valley [19] (Figure 1b). As the main body of the north–south transition zone in China, the climate types in the study area are diverse and exhibit significant vertical changes. The area to the north of Qinling Mountains is mainly affected by the continental climate of the warm temperate zone, which is cool in summer and dry and cold in winter. The area south of Qinling Mountains is mainly affected by the subtropical monsoon climate, which is humid and has four distinct seasons. In addition, the study area includes three types of ecological function protection areas for water conservation, water and soil conservation, and species resources in China (Figure 1c), as well as four forestry projects: the Three North Shelterbelt, the Middle Yellow River Shelterbelt, the Taihang Mountain Greening Project, and the Middle and Upper Yangtze River Shelterbelt (Figure 1d).

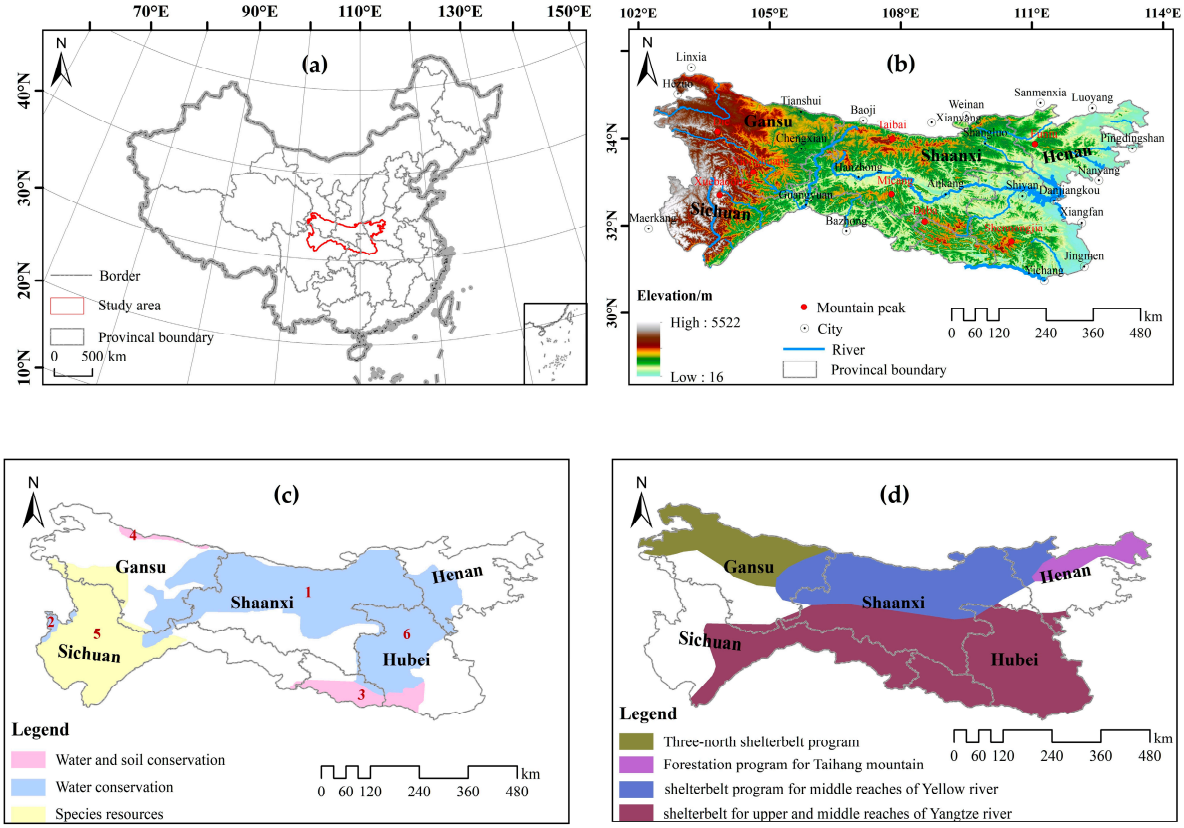

Figure 1. Overview of the QBM: (**a**) Geographical position; (**b**) Basic Elements: elevation, mountain peak, city location, and rivers; (**c**) Ecological Function Reserve (Number 1–6 represent the six ecological function reserves); (**d**) Forestry Engineering.

2.2. Data

The data sources used in this study mainly included MODIS satellite normalized difference vegetation index (MODIS-*NDVI*) data and meteorological station data (temperature, precipitation, and sunshine hours).

2.2.1. NDVI

Remote sensing satellite images provide more possibilities for monitoring vegetation changes in large-scale and long-term time series. The *NDVI* time series data used in this study were obtained from MOD13Q1-*NDVI* data provided by the NASA Land Process Distribution Dynamic Data Center (https://ladsweb.modaps.eosdis.nasa.gov, accessed on 1 September 2020), namely the normalized vegetation index dataset. First, we used the MODIS Reprojection Tool (MRT) to batch extract *NDVI* data and perform splicing, resampling, projection conversion, and other processes to convert them into Tiff images. Second, based on the ENVI platform, the maximum value composites (MVC) method was used to obtain monthly *NDVI* data, and *FVC* data were calculated through the pixel dichotomy model.

2.2.2. Climatic Data

The meteorological data used in this study were obtained from the Daily Data Set of China Surface Climate Data (V3.0) provided by the China Meteorological Data Sharing Service Network (http://cdc.cma.gov.cn, accessed on 1 September 2020). A 50 km buffer zone was created at the boundary of the study area, and the daily average temperature (TEM), precipitation (PRE), and sunshine duration (SSD) data of 100 meteorological stations in the study area and the buffer zone from 2000–2020 were used (Figure 2). Based on the

observation data, ANUSPLIN software was used to conduct spatial interpolation processing on the station data, and grid data of monthly average *TEM*, monthly *PRE*, and monthly *SSD* with a spatial resolution of 250 m were obtained.

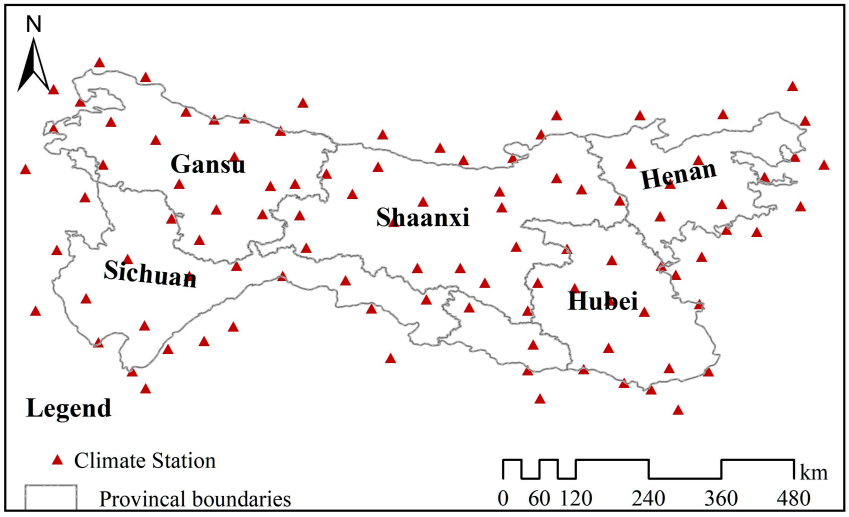

Figure 2. Spatial Distribution of Selected Meteorological Stations in the Study Area.

2.3. Methods

2.3.1. Estimation of Vegetation Coverage

The normalized difference vegetation index (*NDVI*) is the most commonly used vegetation index, and the pixel dichotomy model is the most common linear model used for calculation of vegetation coverage. This model assumes that the information contained in one pixel of a remote sensing image is composed only of vegetation and bare soil [20]. Pixel information includes pure vegetation composition information and pure soil composition information; therefore, the mixed pixel S can be expressed as:

$$S = S_v + S_s \tag{1}$$

where S_v is the vegetation information in the pixel and S_s is the information of bare soil.

The fractional vegetation cover (FVC) of a pixel is the area ratio of the vegetation in the pixel; therefore, the bare soil coverage in the pixel can be expressed as $(1 - FVC)$. Assuming that a pixel with pure vegetation coverage is S_{veg}, the pixel covered by pure bare soil is S_{soil}, then:

$$S_v = FVC \times S_{veg} \tag{2}$$

$$S_s = (1 - FVC) \times S_{soil} \tag{3}$$

If Equations (2) and (3) are introduced into Equation (1), we obtain:

$$FVC = \frac{S - S_{soil}}{S_{veg} - S_{soil}} \tag{4}$$

Therefore, the binary model expression of vegetation coverage pixel based on *NDVI* is as follows:

$$FVC = \frac{NDVI - NDVI_{soil}}{NDVI_{veg} - NDVI_{soil}} \tag{5}$$

The range of *NDVI* is between [−1,1], and negative values indicate that the ground cover is the reflection of visible light by clouds, water, snow. The value 0 indicates the presence of rocks or bare soil. Positive values indicate that there is vegetation cover and they increase with the increase in cover. Therefore, in the calculation of *FVC*, we set the pixels with *NDVI* less than 0 as null values. Theoretically, the value of $NDVI_{soil}$ should be

close to 0, but in fact, it fluctuates within the range of –0.1 to 0.2 owing to different research areas or surface environments. Due to the lack of systematically measured surface data for reference in this study, the *NDVI* statistical histogram is usually given a confidence interval, and the minimum and maximum values within this interval are considered as $NDVI_{soil}$ and $NDVI_{veg}$, or the *NDVI* value of the cumulative frequency [21]. According to the situation of the study area, *NDVI* values of 5% and 95% of the cumulative frequency were considered as $NDVI_{soil}$ and $NDVI_{veg}$. We assigned 0 to values less than 5%, and 1 to values greater than 95%.

To better reflect the distribution and changes in vegetation coverage in the study area, the vegetation coverage was divided into five grades according to the Classification and Grading Standards for Soil Erosion and the specific situation. The results are presented in Table 1.

Table 1. *FVC* Level Classification.

Class	*FVC*	Description
1	≤0.30	Low vegetation coverage
2	(0.30, 0.45]	Sub-low vegetation coverage
3	(0.45, 0.60]	Middle vegetation coverage
4	(0.60, 0.75]	Sub-high vegetation coverage
5	>0.75	High vegetation coverage

2.3.2. Change Trend

Change trend analysis refers to changes in a particular element of the time series (such as *FVC*, *TEM*, *PRE*, and *SSD*) that continuously increase or decrease over a certain period of time [22]. In the present study, the trend analysis method (i.e., least squares method) was used to calculate the interannual change trend of climate elements and *FVC* at different spatial scales, and the slope of the linear regression equation is defined as the interannual change trend rate of elements (slope) [23]. The calculation equation for slope is as follows:

$$Slope = \frac{n \times \sum_{i=1}^{n}(i \times p_i) - \sum_{i=1}^{n} i \times \sum_{i=1}^{n} p_i}{n \times \sum_{i=1}^{n} i^2 - \left(\sum_{i=1}^{n} i\right)^2} \quad (6)$$

where n is the total year of the study period, i is the serial number of each year, p_i is the pixel value of the i-th year, and *Slope* is the change in slope of the data on each pixel time series. When $Slope > 0$, it indicates that the pixel value increases with time; that is, it shows an improvement trend during the study period. When $Slope = 0$ indicates no change, and when $slope < 0$, the pixel value decreases with time; that is, it shows a degradation trend. The greater the absolute value of *Slope*, the greater is the change rate of the elements. Combined with the significant results of the t test, the change trend was divided into the following five levels, as shown in Table 2.

Table 2. Classification of change trend level.

Class	Slope	*p* Value	Description
1	>0	<0.05	Significant increase
2		>0.05	No significant increase
3	<0	<0.05	Significant decrease
4		>0.05	No significant decrease
5	=0	-	No changed

2.3.3. Correlation Analysis

To analyze the relationship between *FVC* and climate elements, it is necessary to establish a simple correlation coefficient between them on a pixel scale. This correlation coefficient, also known as the Pearson correlation coefficient, is widely used to measure

the correlation between two variables, and its value is between −1 and 1. The calculation equation is as follows:

$$R = \frac{\sum_{i=1}^{n}\left[\left(x_i - \overline{X}\right)\left(y_i - \overline{Y}\right)\right]}{\sqrt{\sum_{i=1}^{n}\left(x_i - \overline{X}\right)^2 \sum_{i=1}^{n}\left(y_i - \overline{Y}\right)^2}} \quad (7)$$

where R is the correlation coefficient; n is the number of samples; x_i, y_i are the variables to be evaluated; and $\overline{X}$ and $\overline{Y}$ are, respectively, the mean of x_i and y_i. If $R > 0$, there is a positive correlation between the two; otherwise, it indicates a negative correlation. The closer the absolute value of R is to 1, the closer is the correlation between x and y; the closer the absolute value of R is to 0, the less close is the correlation between them. The correlation level can be classified into five types (Table 3).

Table 3. Classification of correlation level.

Class	R	*p* Value	Description
1	>0	<0.05	Significant positive correlation
2		>0.05	No significant positive correlation
3	<0	<0.05	Significant negative correlation
4		>0.05	No significant negative correlation
5	=0	-	No correlation

2.3.4. Relative Importance

When analyzing the impact of multiple elements on a single element, we must pay attention to the relative importance of each element. The calculation of relative importance was based on standardized coefficients or variance interpretation. Based on raster data from a long time series, the present study uses a multiple regression analysis method. First, a multiple linear regression model between *FVC* and climate factors was developed to explain the influence of multiple climate factors changes on *FVC* using *TEM*, *PRE*, and *SSD* as independent variables and *FVC* as a dependent variable.

The equation used was as follows:

$$FVC = A \times TEM + B \times PRE + C \times SSD + d \quad (8)$$

where A, B and C are regression coefficients of the three climatic elements, and d is a constant.

Secondly, in order to better identify the most important climate factors affecting the *FVC* variation in each pixel, we standardized the coefficients of the multiple regression model. The maximum absolute value of the standardized regression coefficient is considered as the most important variable. The formula for standardization was as follows:

$$\begin{aligned} A' &= A \times \frac{std(TEM)}{std(FVC)} \\ B' &= B \times \frac{std(PRE)}{std(FVC)} \\ C' &= C \times \frac{std(SSD)}{std(FVC)} \end{aligned} \quad (9)$$

where A', B', C' represent the normalization factors of *TEM*, *PRE*, and *SSD*.

3. Results

3.1. Spatiotemporal Changes of FVC

3.1.1. Time Variation

Figure 3a shows the overall trend of annual average *FVC* in the QBM from 2000–2020. In the past 21 years, the vegetation coverage of the QBM improved continuously, and increased significantly at a rate of 0.058/10a ($p < 0.01$). From 2011–2020, the annual growth rate of *FVC* was faster than that of the previous 11 years.

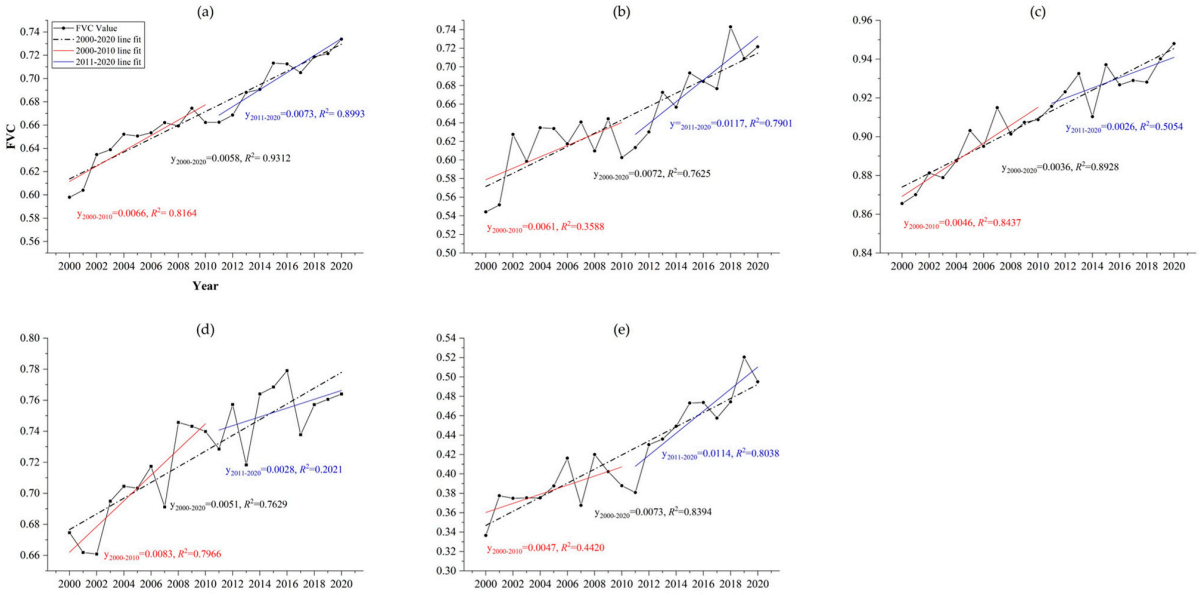

Figure 3. Change of *FVC* average value in the QBM from 2000–2020. (**a**) Year; (**b**) Spring; (**c**) Summer; (**d**) Autumn; (**e**) Winter.

The growth of surface vegetation generally exhibits a certain periodicity (Figure 3b,e). The growth rate in summer was the slowest, but the fastest in winter, and the growth rate of the *FVC* average value in spring was faster than that in autumn.

3.1.2. Spatial Pattern Change

In terms of spatial distribution, the annual average *FVC* value of the QBM was higher in the south, lower in the north, and lower in the east and west than in the middle (Figure 4a). Most areas are at a sub-high or high vegetation coverage level (Figure 4b). The high-value (>0.75) was mainly distributed in Daba Mountains and Qinling Mountains in Shaanxi, whereas the low-value (<0.30) area is very small and scattered in northwest Sichuan. The average values of *FVC* in Chongqing, Hubei, and Shaanxi were larger (>0.70), and in Henan and Gansu they were the smallest. This shows that the vegetation coverage in most areas has been in a good state over the past 21 years, especially in Daba Mountains and surrounding areas.

Spatially, the annual change trend rate generally showed increasing distribution characteristics from southwest to northeast (Figure 4c). The vegetation coverage in most regions of the QBM has significantly improved over the past 21 years, and the regions with faster growth rate (>0.06/10a) were concentrated in Shaanxi, Gansu, and Chongqing (Table 4). From the perspective of space, these areas have a good basis for vegetation coverage and are also key implementation areas for forestry projects, such as returning farmland to forests and grasslands. Less than 3% of the regional average annual *FVC* showed a downward trend, scattered across in Chengdu, Aba, Hanzhong, Shiyan, and Luoyang. The growth and development of vegetation in these areas may be affected by altitude or population distribution.

The spatial pattern of the *FVC* average in each season was similar to the annual average (Figure 5a); however, there were regional differences in the *FVC* trend in different seasons (Figure 5c). The average *FVC* in spring at the sub-high vegetation coverage level (Figure 5b) and the vegetation cover were significantly improved. The significantly improved area was distributed within Shaanxi, especially in Ankang and Shangluo; the decrease trends were scattered across Tianshui and Hanzhong. Spatially, the trend rate showed a distribution feature of increasing from both sides to the central region. The average change trend rate of each region was between 0.060/10a and 0.087/10a, with Chongqing and Shaanxi being the fastest and Sichuan the slowest.

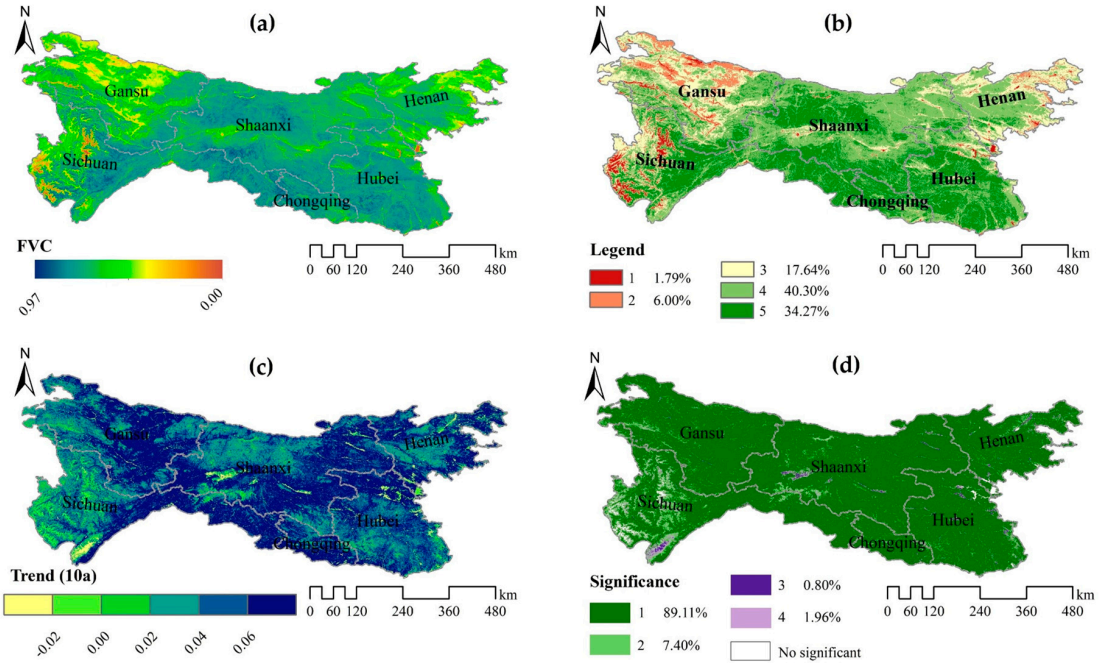

Figure 4. Changes of *FVC* spatial pattern in the QBM from 2000–2020. (**a**) Average value; (**b**) *FVC* level; (**c**) Change trend rate; (**d**) Significance level.

Table 4. Annual average vegetation coverage and trend rate in the QBM.

	FVC					Slope/10a				
	Year	**Spring**	**Summer**	**Autumn**	**Winter**	**Year**	**Spring**	**Summer**	**Autumn**	**Winter**
QB	0.67	0.64	0.91	0.73	0.42	0.058	0.072	0.036	0.051	0.073
SC	0.69	0.63	0.91	0.74	0.48	0.050	0.060	0.019	0.040	0.075
SX	0.72	0.71	0.95	0.78	0.44	0.060	0.081	0.031	0.045	0.081
HB	0.73	0.72	0.94	0.78	0.47	0.056	0.070	0.026	0.051	0.074
HN	0.59	0.58	0.85	0.64	0.29	0.057	0.073	0.043	0.058	0.057
GS	0.58	0.52	0.86	0.64	0.32	0.065	0.070	0.065	0.065	0.058
CQ	0.76	0.73	0.94	0.82	0.55	0.067	0.087	0.028	0.055	0.095

(SC, SX, HB, HN, GS and CQ are abbreviation for Sichuan, Shaanxi, Hubei, Hunan, Gansu, and Chongqing provinces, respectively).

Most areas in summer had high vegetation coverage. A small number of low-value areas were distributed in Aba, Sichuan. In 21 years, the area with a positive trend rate of average *FVC* change in summer accounted for the least (84.93%), and the faster increase rate were mainly in the east and west of the Qinling Mountains. Compared with other seasons, the area proportion of *FVC* showing a downward trend in summer was larger (10.62%) and was mainly distributed in western Sichuan and southern Shaanxi, but the significance of this decline in most regions was weak. The average change trend rate of *FVC* in each region in summer was between 0.019/10a and 0.065/10a, and the fastest and slowest were Gansu and Sichuan, respectively.

The spatial distribution of *FVC* in autumn was consistent with that in spring, and it was also at the sub-high vegetation coverage level overall. Approximately 7% of regions with a decreasing trend were concentrated in Deyang and Aba. The regional proportion of *FVC* showing a very significant upward trend was 62.53%, mainly distributed in Gansu and eastern regions. The average change trend rate of regional *FVC* was within the range of 0.040/10a–0.065/10a, and the fastest and slowest rates remained in Gansu and Sichuan, respectively.

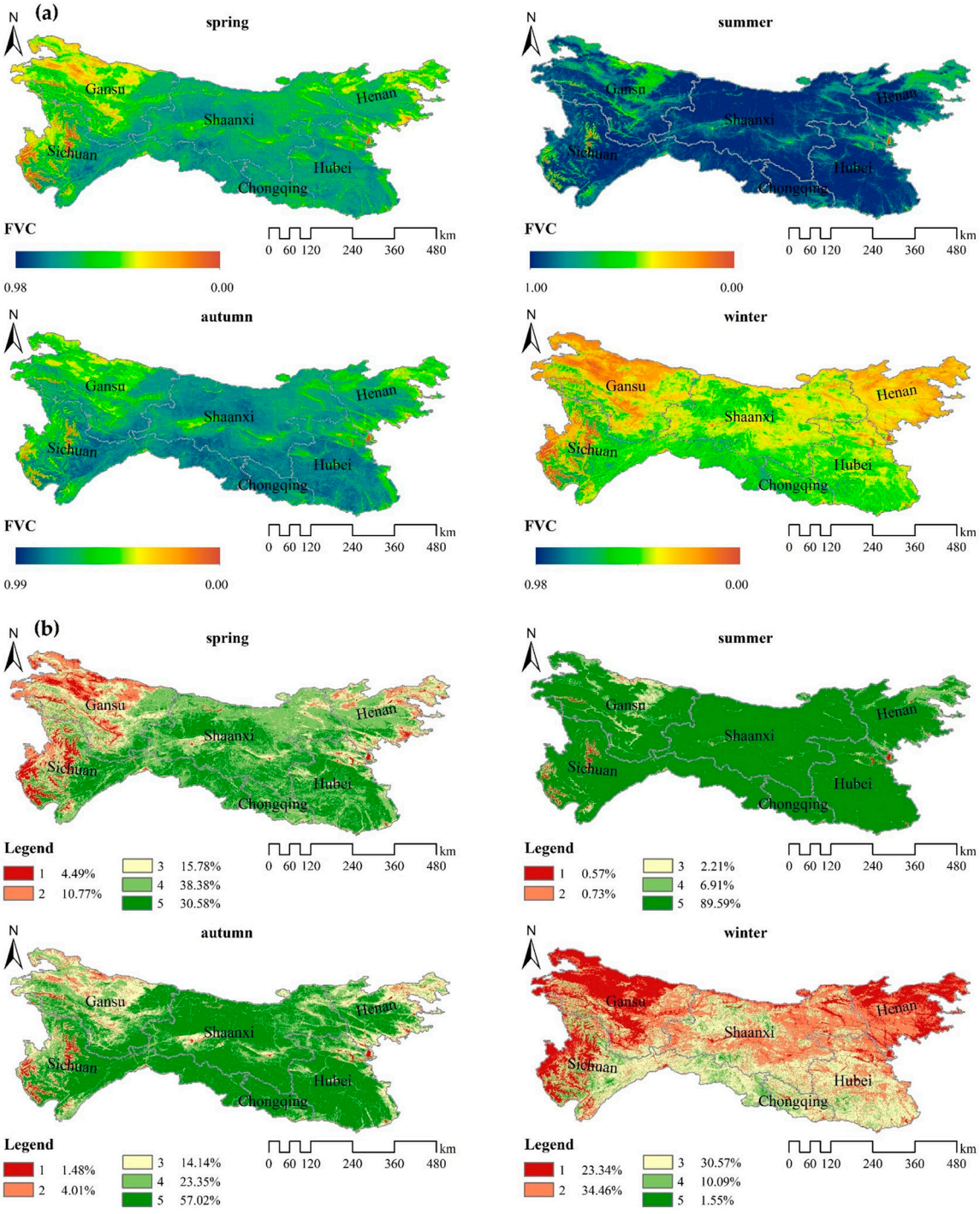

Figure 5. *Cont.*

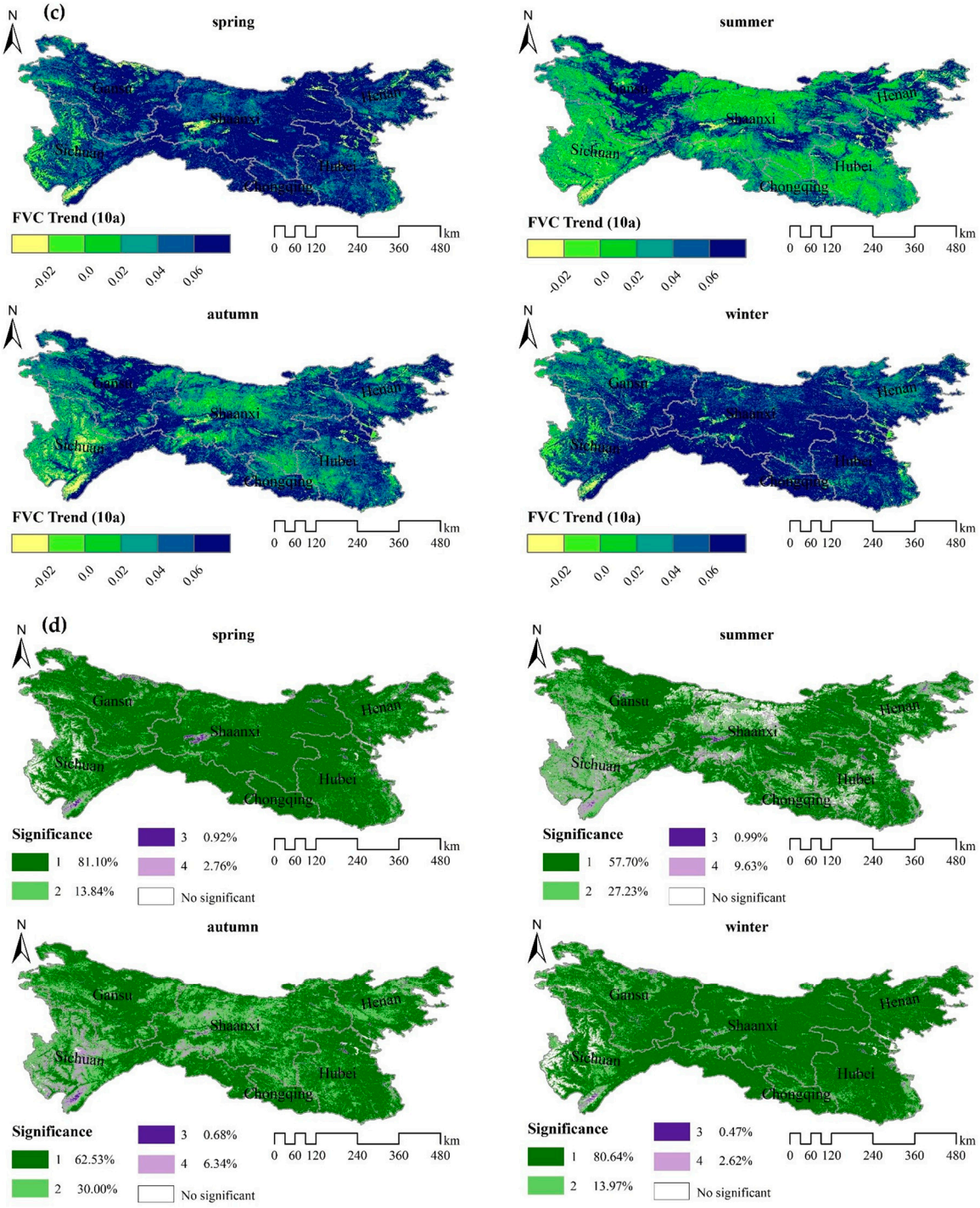

Figure 5. Change of seasonal average *FVC* spatial pattern in the QBM from 2000–2020. (**a**) Average value; (**b**) *FVC* level; (**c**) Change trend rate; (**d**) Significance level.

The average *FVC* value in winter was the lowest, which is generally at the sub-low vegetation coverage level. The low-value areas were concentrated in the west and northeast, while the high-value areas were few and scattered around Daba Mountains. The change trend rate of *FVC* in winter is close to that in spring; Chongqing and Henan had the fastest and slowest values, respectively. In addition, the area proportion of *FVC* increasing or decreasing was also similar to that in spring. The difference was that in winter, the *FVC*

in the western region showed a downward trend, whereas that in Hanzhong showed an upward trend.

In general, vegetation coverage in the QBM was low only in winter and high in the other seasons. During the 21 years, the vegetation coverage in most areas improved in each season, but the improvement rate had a certain heterogeneity. The seasonal average *FVC* change trend rate in Sichuan, Shaanxi, Hubei, and Chongqing decreased and then increased. The minimum trend rate appeared in summer and, the maximum in winter; while in spring, it was faster than that in autumn. This trend was contrary to that of the average *FVC* in each season. In contrast, the trend rate of seasonal average *FVC* in Henan and Gansu showed a trend to "decrease-increase-decrease." The minimum value appeared in summer, while the maximum value occurred in spring.

3.2. Spatiotemporal Changes of Climate Factors

3.2.1. Time Variation

In the last 21 years, the annual average *TEM* in the QBM has been 10.12 °C, rising at a rate of 0.175 °C/10a (Figure 6a). However, since 2016, the average annual *TEM* has decreased by approximately 0.3 °C. This indicates that during the study period, the QBM also experienced a "warming" trend, especially in the past 10 years, when the *TEM* increased significantly; but in the past five years, "cooling" was observed. The growth rate of the average *TEM* in summer and autumn was higher, whereas that in winter was the slowest and showed a weak downward trend. The growth rate/deceleration was fastest in autumn/winter before 2010, and faster in winter and spring after 2010 (Figure 7a).

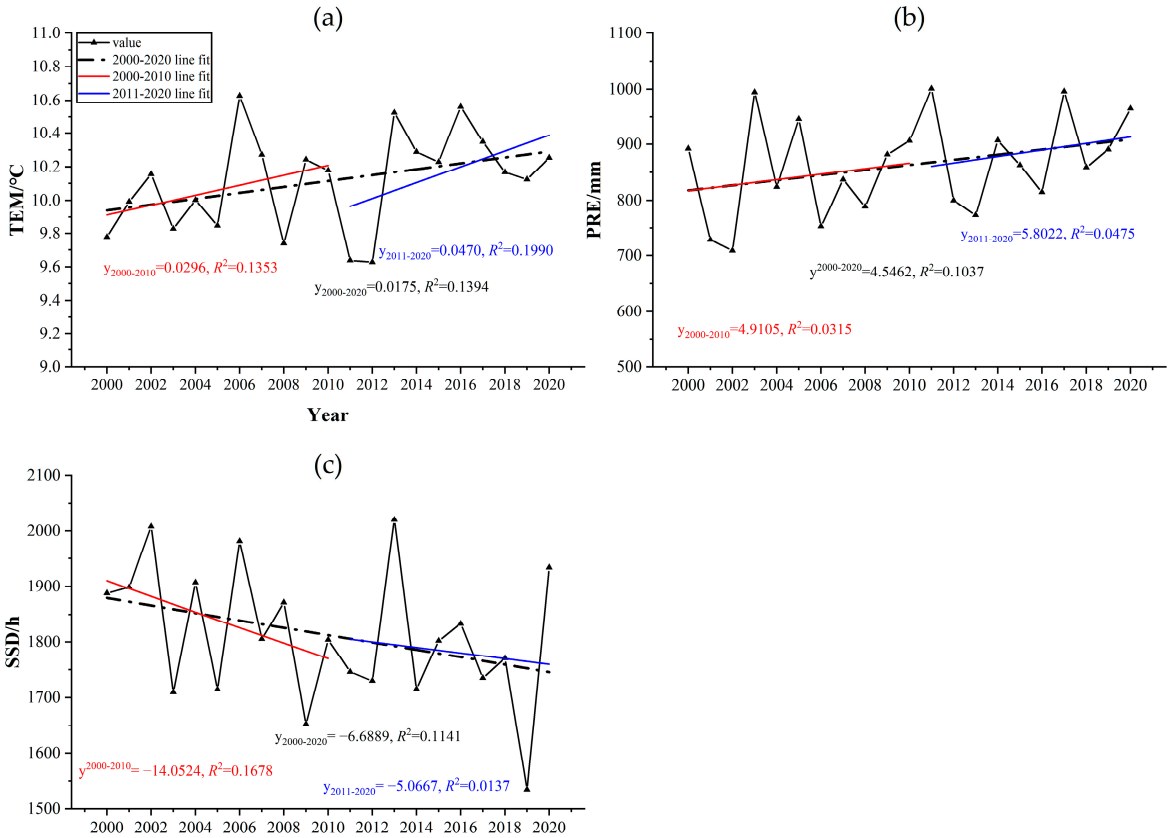

Figure 6. Annual mean change of climate factors in the QBM from 2000–2020: (**a**) *TEM*; (**b**) *PRE*; (**c**) *SSD*.

Figure 6b shows that the annual *PRE* has increased at a rate of 45.46 mm/10a in the past 21 years. Similar to the annual average *TEM*, the average value and increase rate of annual *PRE* before 2010 were smaller than those after 2010. The *PRE* in summer was the

largest, slightly lower in spring than in autumn, and the lowest in winter (Figure 7b). In all four seasons, the growth rate was fastest in spring, particularly before 2010; the next was autumn and summer, and their rate of change was faster after 2010. Generally, there was a slight downward trend in winter.

In contrast to the *TEM* and *PRE*, the annual *SSD* showed a gradual downward trend at a rate of 66.89 h/10a during the study period (Figure 6c), and the decline rate in the first 11 years was 2.8 times that in the next 10 years. According to the seasonal average, the *SSD* in summer and spring was longer, followed by winter and autumn. Seasonally, spring and autumn showed a decreasing trend, summer and winter showed an increasing trend, and the fall/rise speed was faster in autumn/winter. However, it was found that the rate of decline in spring and summer was faster in 2000–2010, being fastest in autumn, whereas it was the fastest in winter in 2011–2020.

3.2.2. Spatial Pattern Change

From 2000–2020, the annual average *TEM* of the QBM was generally distributed in the zonal direction, that is, the spatial distribution characteristics of gradual increase from northwest to southeast (Figure 8(a1)). The low-value was concentrated in the western Songpan Plateau, whereas the high-value was mainly distributed in the eastern plain. Among them, Hubei and Henan had the highest, Gansu had the lowest (Table 5). Spatially, the heating rate generally increased from the central regions to both sides (Figure 8(a2)). The cooling areas were mainly distributed in the south, Guangyuan and Yichang, but the significance was weak. The regions that warmed faster (>0.60 °C/10a) and passes the significance level test were located mainly in Gannan, Luoyang, and Zhengzhou. In all regions, the fastest average warming rate was in Henan, and the slowest was in Shaanxi.

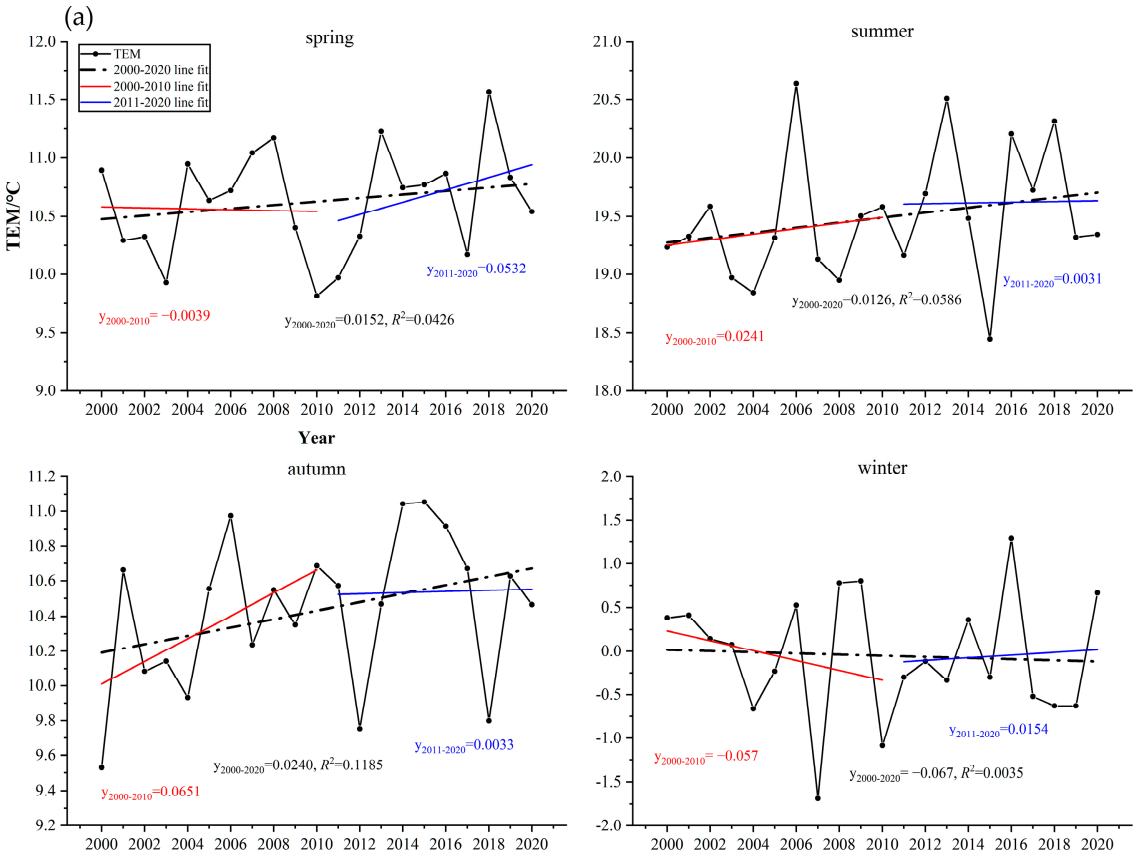

Figure 7. *Cont.*

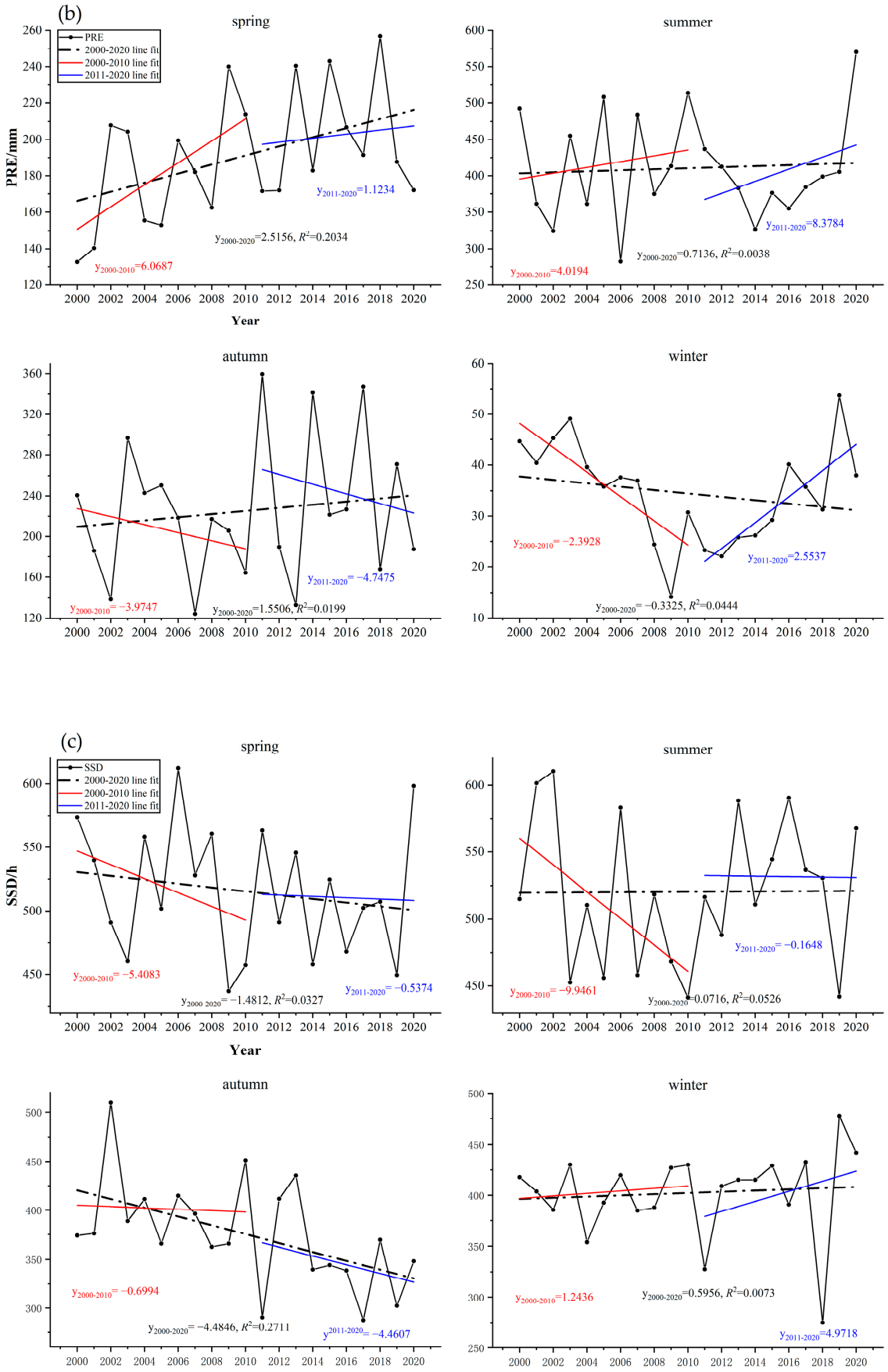

Figure 7. Seasonal mean changes of climate factors in the QBM from 2000–2020: (**a**) *TEM*; (**b**) *PRE*; (**c**) *SSD*.

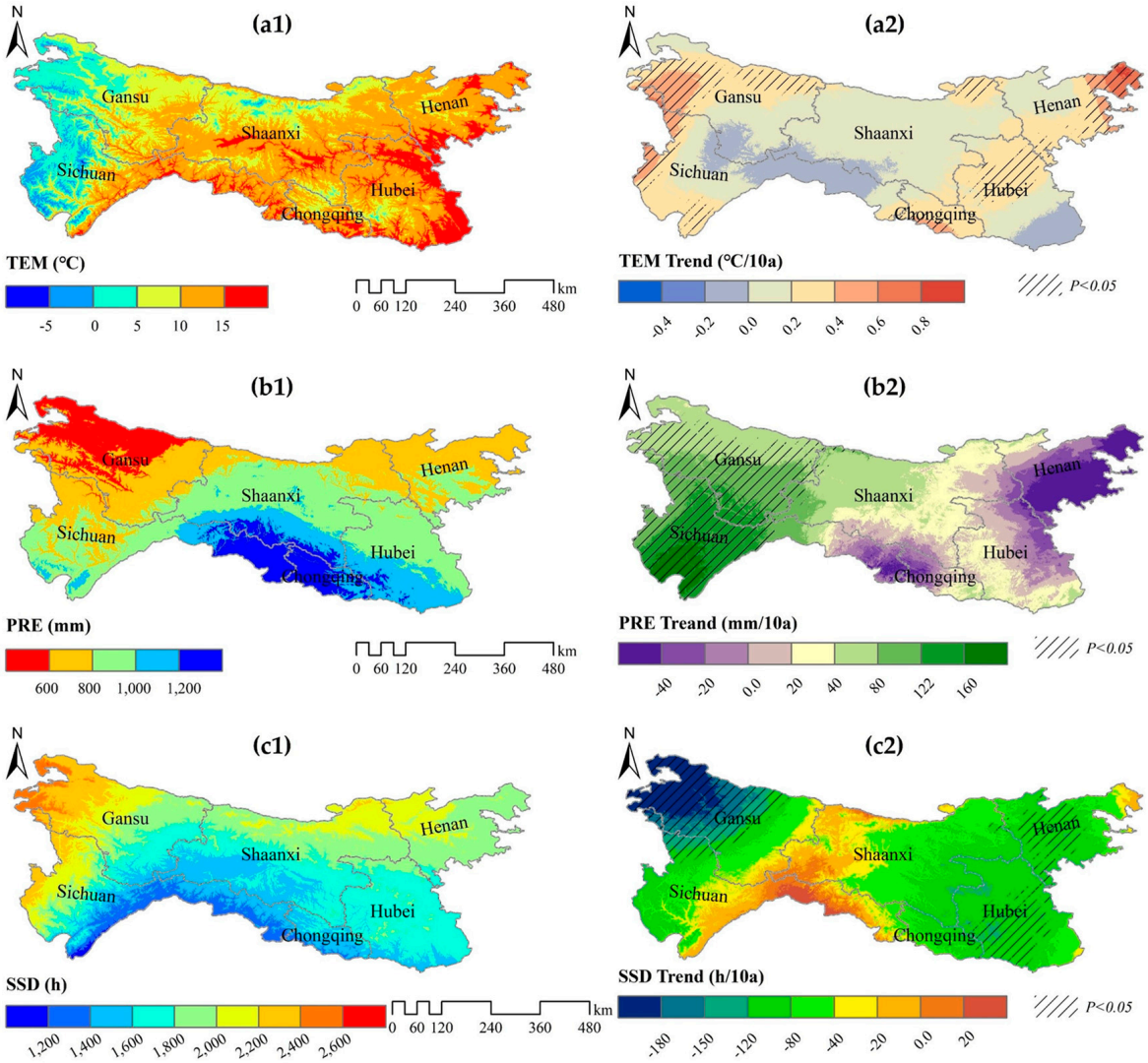

Figure 8. The spatial pattern changes of climate factors in the QBM from 2000–2020: (**a**) *TEM*; (**b**) *PRE*; (**c**) *SSD*. (1. Annual average; 2. Change trend rate).

Table 5. Annual average and change trend rate of climate factors in the QBM.

	Average Value			Slope/10a		
	TEM/°C	*PRE*/mm	*SSD*/h	*TEM*/°C	*PRE*/mm	*SSD*/h
QB	10.12	863.26	1812.51	0.175	45.462	−66.885
SC	7.50	925.20	1702.18	0.139	103.575	−48.757
SX	11.01	916.69	1779.01	0.118	39.114	−56.645
HB	13.54	976.99	1707.04	0.150	9.929	−101.508
HN	13.11	754.91	1949.17	0.307	−36.342	−87.147
GS	6.81	626.26	2028.31	0.208	81.862	−124.771
CQ	11.97	1255.14	1526.85	0.292	1.232	−83.292

Figure 8(b1) shows that the annual *PRE* was generally characterized by a gradual decrease in spatial distribution from southeast to northwest. The average annual *PRE* in Chongqing was the largest, whereas that in Gansu was the smallest. The annual *PRE* change rate of increase is generally characterized by its distribution increasing from east to west (Figure 8(b2)). In the past 21 years, the regions with reduced *PRE* were concentrated around the mountains of western Henan and Daba Mountains but did not pass the significance test. The faster (>160 mm/10a) increase trend rate was mainly distributed in the southwest,

such as in Maoxian, Sichuan. The regional average annual *PRE* growth rate was the largest in Sichuan and the smallest in Henan.

The spatial distribution of annual *SSD* generally increases with increasing latitude, that is, it is low in the south and high in the north. High values of annual *SSD* are mainly distributed in the northwest, whereas the low-value area was concentrated in the northern edge of Sichuan Basin. Gansu and Henan have the largest value, and Chongqing has the smallest value. Figure 8(c1) shows that the annual *SSD* in most regions is decreasing. The increasing trend was concentrated in the northern edge of Sichuan Basin, while the decreasing trend was in the northwest, including Dingxi, Gannan and Linxia.

In summary, the west of the QBM was cold and dry with ample sunshine. The south was warm and humid, but the *SSD* was short. Most areas in the north were warm and dry with long *SSD*. However, these characteristics have changed over the past 21 years. The western region is gradually warming and humidifying, whereas the *SSD* is significantly reduced. In the southern region, *TEM* and humidity have decreased, but *SSD* has begun to increase. *TEM*, *PRE*, and *SSD* in the north show a weak increase/decrease trend.

In the past 21 years, the spatial distribution characteristics of the average *TEM* in each season showed a gradual increase from west to east. The spatial difference of average *TEM* in summer was the largest, the maximum value between east and west was more than 25 °C (Figure 9a). The annual average *TEM* in each season was 10.63 °C, 19.49 °C, 10.43 °C and −0.05 °C in spring, summer, autumn, and winter, respectively (Table 6). Gansu had the lowest average *TEM* in spring, autumn and winter, and Shaanxi had the lowest average *TEM* in summer, whereas Henan had the highest in spring and summer, and Hubei and Chongqing had the highest in autumn and winter.

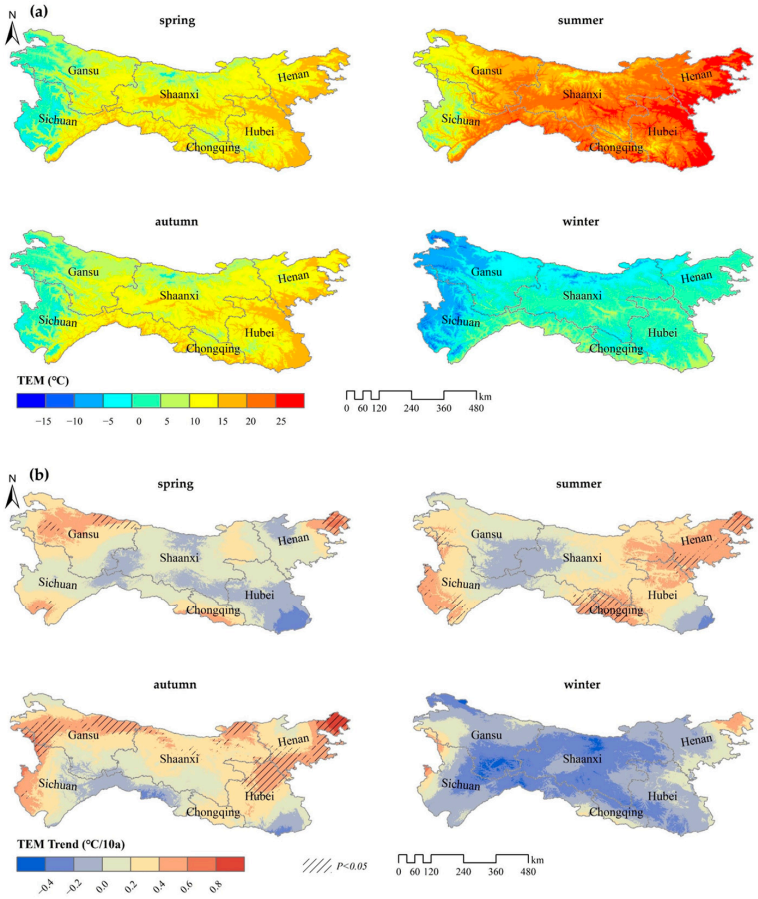

Figure 9. Change of seasonal average *TEM* spatial pattern in the QBM from 2000–2020. (**a**) Seasonal average; (**b**) Seasonal change trend rate.

Table 6. Seasonal average and change trend rate of *TEM* in the QBM.

		Average Value				Slope (°C/10a)			
		Spring	**Summer**	**Autumn**	**Winter**	**Spring**	**Summer**	**Autumn**	**Winter**
TEM	QB	10.63	19.49	10.43	−0.05	0.15	0.22	0.24	−0.07
	SC	7.75	15.55	8.04	−1.32	0.17	0.26	0.16	−0.10
	SX	11.62	20.74	11.12	0.64	0.07	0.20	0.25	−0.25
	HB	13.87	23.32	14.06	2.98	−0.04	0.23	0.23	−0.10
	HN	14.03	23.82	13.33	1.30	0.18	0.45	0.42	0.05
	GS	7.49	16.07	7.03	−3.35	0.29	0.11	0.30	−0.14
	CQ	11.95	20.79	12.59	2.72	0.27	0.47	0.23	−0.09

The variation in average *TEM* in each season exhibited spatial heterogeneity. Most areas showed a warming trend in all seasons except for winter (Figure 9b). The *TEM* dropped in spring, mainly in the junction of Gansu, Shaanxi, and Sichuan, and south of the Han River. In summer, the cooling area was still concentrated at the junction of Gansu, Shaanxi, and Sichuan, the trend rate changed from negative to positive, and the diffusion increased from this central area. The autumn cooling areas were concentrated in the south, especially in Sichuan. The average *TEM* in winter showed a downward trend overall, and the warming trend was mainly to the east and west.

From a regional perspective, the seasonal average *TEM* in Sichuan, Henan, Hubei, and Chongqing, as for *FVC*, initially experienced an increasing but then decreased. The maximum and minimum trend rates occurred in summer and winter, respectively. Although Shaanxi initially increased and then decreased, the maximum trend occurred in autumn. The change in trend rate in Gansu alternated from a change of decrease to increase to decrease, with the maximum appearing in autumn and the minimum in winter.

The seasonal *PRE* in the QBM generally shows a decreasing spatial distribution from southeast to northwest (Figure 10a). The *PRE* values were the most abundant in summer and the spatial difference was the largest, reaching more than 400 mm. In contrast, the *PRE* was rare in winter, and the spatial difference was the least. The distribution of *PRE* in spring and autumn was similar in the western region, but in the central and eastern regions, it was lower in spring than in autumn. Chongqing had the largest regional *PRE* in each season, Henan had the lowest *PRE* in spring, and Gansu had the lowest *PRE* in other seasons (Table 7).

Figure 10b shows that the trend rate of the *PRE* in spring was positive and gradually increased from four sides to the central region. The regions with increased and decreased summer *PRE* presented a spatial pattern of opposite distributions. In the area west of Shangluo-Ankang-Bazhong, the summer *PRE* showed an increasing trend, and the growth rate in the south was higher than that in the north. The area to the east showed a decreasing trend, and the rate of decrease shrank from the center to the northwest and southeast. In autumn, the *PRE* shows an increasing trend in most areas. The downward trend was mainly distributed in Gansu, central Sichuan, western Shaanxi, and central Henan. The rate of change of winter *PRE* gradually decreased from northwest to southeast. Only the northwest region exhibited a weak increasing trend.

From a regional perspective, the trend rate of seasonal *PRE* change in Shaanxi, Hubei, Henan, and Chongqing was characterized by a decrease-increase-decrease. The minimum value appeared in summer, and the maximum value in autumn. Sichuan and Gansu were characterized by first increasing and then decreasing, with the maximum in summer and the minimum in winter.

In the past 21 years, the *SSD* in the QBM has been long in spring and summer; and short in autumn and winter (Table 8). Spatially, the change along the latitude generally decreased from north to south (Figure 11a). The spatial difference was the largest in winter, reaching more than 450 h, and the smallest in summer. In terms of different regions,

in Sichuan and Chongqing, *SSD* was relatively short, and in Henan and Gansu it was relatively long.

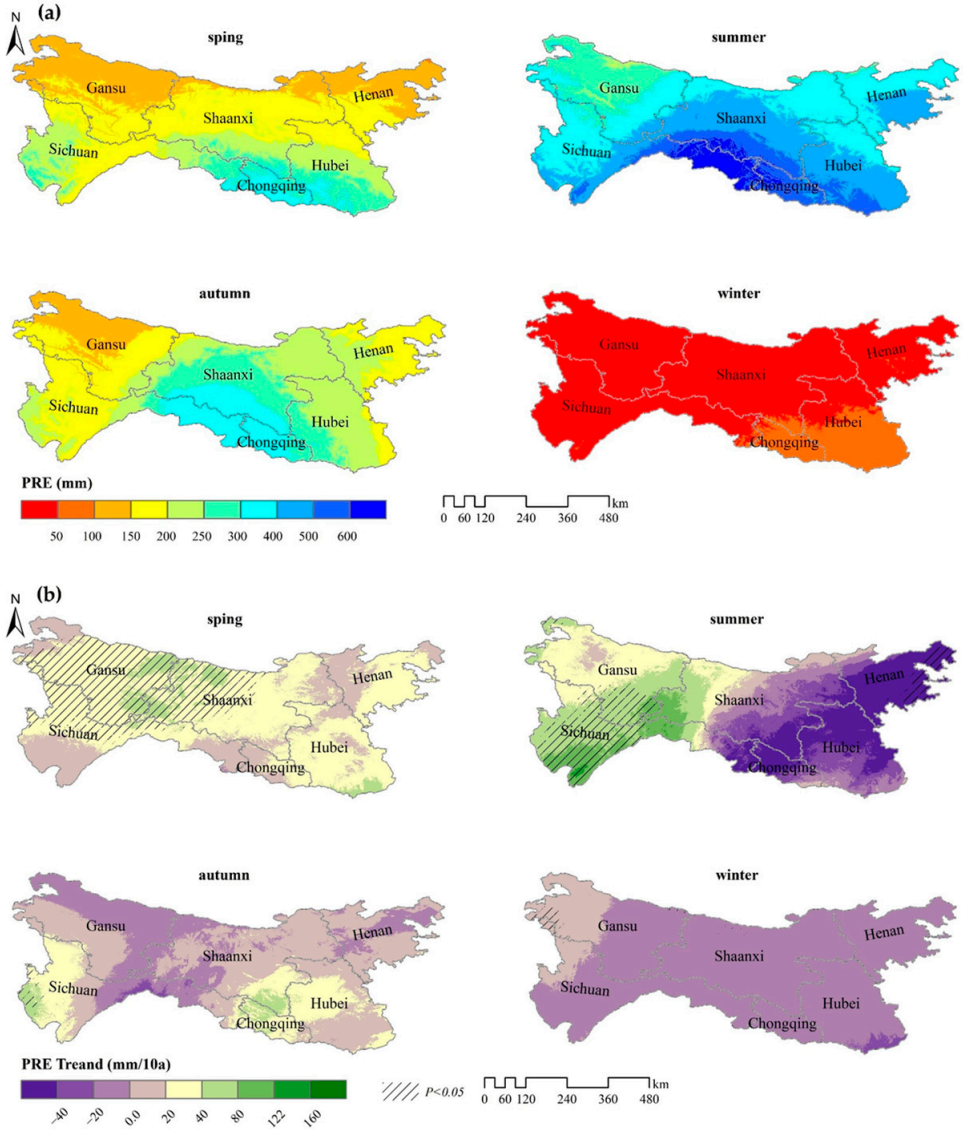

Figure 10. Change of seasonal average *PRE* spatial pattern in the QBM from 2000–2020. (**a**) Seasonal average; (**b**) Seasonal change trend rate.

Table 7. Seasonal average and change trend rate of *PRE* in the QBM.

		Average Value				Slope (°C/10a)			
		Spring	**Summer**	**Autumn**	**Winter**	**Spring**	**Summer**	**Autumn**	**Winter**
PRE	QB	191.28	410.50	225.31	34.49	25.16	7.14	15.51	−3.33
	SC	215.17	446.09	232.55	27.61	22.72	53.23	14.76	−1.89
	SX	185.44	436.14	264.00	33.56	29.65	1.62	7.30	−4.89
	HB	239.92	441.49	232.29	58.01	25.88	−36.50	19.54	−11.19
	HN	140.73	382.76	192.44	39.03	22.29	−63.85	2.75	−6.37
	GS	143.21	304.00	158.43	16.85	30.31	39.94	−1.32	−0.44
	CQ	311.38	552.02	331.33	60.67	19.32	−39.93	33.06	−7.85

Table 8. Seasonal average and change trend rate of *SSD* in the QBM.

		Average Value				Slope (°C/10a)			
		Spring	**Summer**	**Autumn**	**Winter**	**Spring**	**Summer**	**Autumn**	**Winter**
SSD	QB	515.66	520.55	375.43	402.28	−14.81	0.72	−44.85	5.96
	SC	465.32	461.86	364.47	413.70	−5.76	10.63	−32.48	12.22
	SX	519.31	540.01	347.59	371.90	−20.57	20.48	−40.60	24.90
	HB	481.35	520.23	368.53	337.14	−30.93	4.22	−51.62	8.97
	HN	583.11	530.99	418.72	417.47	−42.40	9.95	−51.85	23.49
	GS	568.03	549.34	414.26	498.82	−16.88	−36.82	−49.52	−2.27
	CQ	419.90	514.51	325.74	271.79	−19.72	13.81	−47.41	13.48

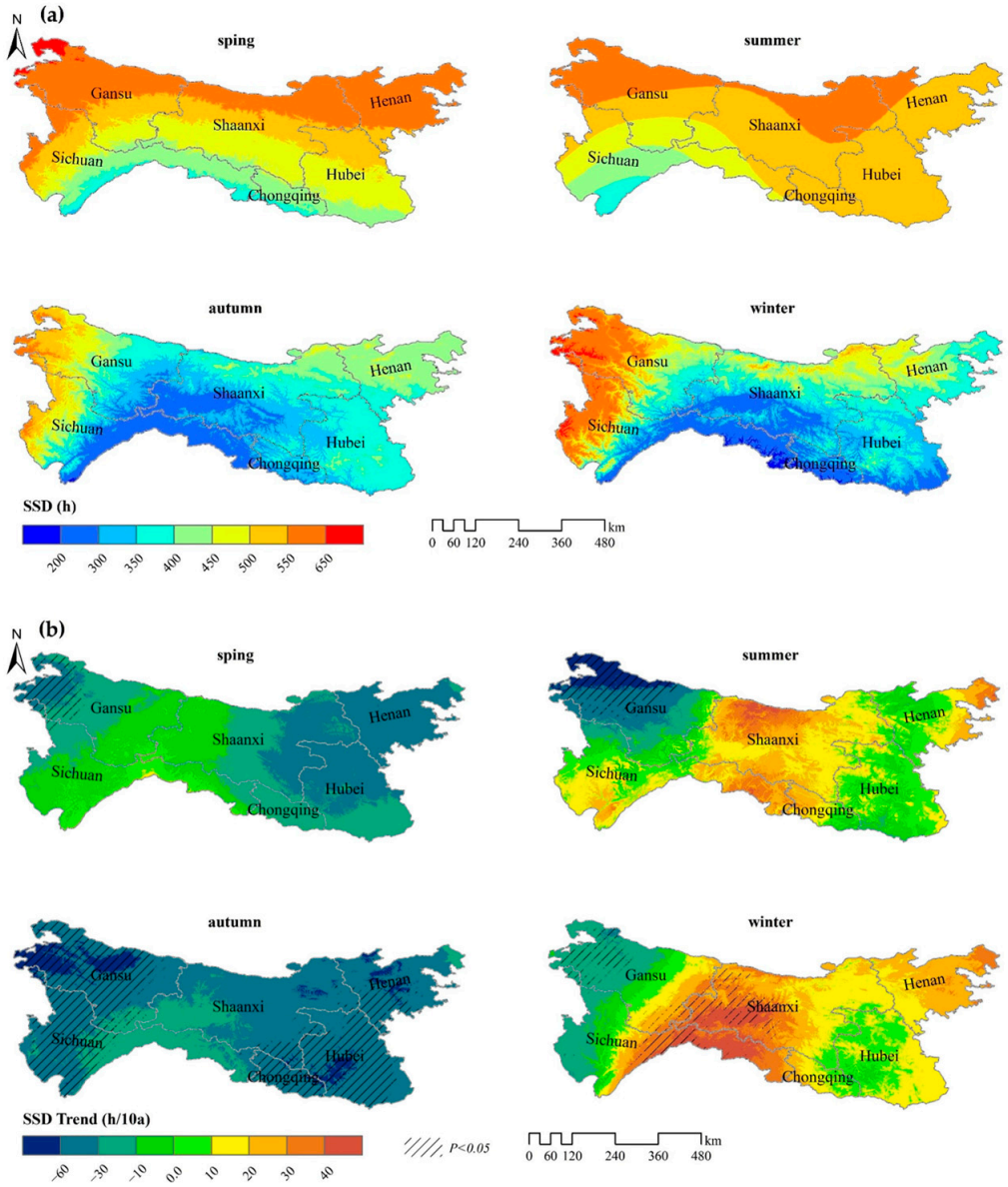

Figure 11. Change of seasonal average *SSD* spatial pattern in the QBM from 2000–2020. (**a**) Seasonal average; (**b**) Seasonal change trend rate.

The change trend rate of *SSD* in the four seasons showed clear spatial differences. The *SSD* in spring generally showed a decreasing trend, and the trend rate decreased from the center to both sides. A small increase was mainly in the south at the edge of Sichuan Basin (Figure 11b). In summer, decreases and increases in *SSD* were distributed interactively; and

decrease were mainly on the east and west sides; and increases were in the central area, Qinling Mountains in Shaanxi, and Daba Mountain area, which exhibited the fastest growth rate. Similar to spring, *SSD* in autumn also decreased. The regions with the fastest decline rate were mainly in northern Gansu, central Henan, and the areas around Shennongjia in Hubei. In winter, the *SSD* in most areas increased and the growth rate in the center was the fastest. The areas with reduced *SSD* were concentrated in the west.

In Sichuan, Shaanxi, Hubei, Henan, and Chongqing, the rate of change of *SSD* in each season was consistent, showing a "N" pattern, with the maximum in winter and the minimum in autumn. The rate of change showed a "V" pattern, only in Gansu, with the maximum appearing in winter and the minimum in autumn.

3.3. Response of FVC Change to Climatic Factors

3.3.1. Response of *FVC* Change to a Single Climate Factor

The correlation coefficients between the annual, and seasonal average *FVC* and average *TEM*, *PRE*, and *SSD* were calculated (Table 9). Overall, from 2000–2020, the annual average *FVC* of the QBM was positively correlated with *TEM* and *PRE* but negatively correlated with *SSD*, with the correlation with *TEM* being stronger than those with *PRE* and *SSD*. From the perspective of each season, *FVC* was positively correlated with average *TEM*, with the strongest correlation in spring. The *FVC* was positively correlated with *PRE* in all seasons except winter. In contrast to *PRE*, only *SSD* in winter had a weak positive correlation with *FVC* and the other seasons had a negative correlation, with the maximum value appearing in autumn. The above results show that the vegetation coverage in the QBM is greatly affected by *TEM*, whereas the influence of *PRE* and *SSD* is relatively weak. However, in spring, the impact of *PRE* may be more obvious than that of the average *TEM*, whereas in autumn and winter, it is more affected by *SSD*.

Table 9. Correlation coefficient between *FVC* and climatic factors in the QBM.

		QB	SC	SX	HB	HN	GS	CQ
Year	*TEM*	0.26	0.22	0.24	0.29	0.25	0.32	0.41
	PRE	0.18	0.25	0.09	0.10	−0.05	0.44	0.09
	SSD	−0.20	−0.01	−0.05	−0.33	−0.36	−0.39	−0.23
Spring	*TEM*	0.22	0.25	0.21	0.10	0.07	0.36	0.37
	PRE	0.35	0.26	0.35	0.37	0.27	0.50	0.27
	SSD	−0.10	0.04	−0.03	−0.20	−0.34	−0.08	−0.10
Summer	*TEM*	0.04	0.03	0.08	0.06	0.14	−0.06	0.09
	PRE	0.05	0.06	−0.02	−0.03	−0.08	0.29	0.00
	SSD	−0.05	0.13	0.01	−0.08	−0.06	−0.26	−0.03
Autumn	*TEM*	0.19	0.18	0.22	0.17	0.05	0.25	0.22
	PRE	0.09	0.09	0.03	0.09	0.16	0.14	0.21
	SSD	−0.24	−0.14	−0.13	−0.30	−0.29	−0.38	−0.33
Winter	*TEM*	0.09	0.06	0.03	0.08	0.23	0.13	0.11
	PRE	−0.09	−0.11	−0.11	−0.01	0.00	−0.16	0.05
	SSD	0.15	0.21	0.20	0.05	0.07	0.13	0.26

Figure 12 shows the spatial distribution of the correlation between the annual average *FVC* and the annual average *TEM*, *PRE*, and *SSD* in the QBM from 2000–2020. Over the 21 years, there was a positive correlation between the annual average *FVC* and the annual average *TEM* in nearly 90% of the regions (Table 10), especially in the south of Gansu and northeast of Henan. A generally weak negative correlation was mostly observed in the southern region, Guangyuan; however, the negative correlation was generally weak (Figure 12a). This shows that the increase in *TEM* in most parts of the study area over the past 21 years was conducive to the growth and development of vegetation, thereby promoting an improvement in regional vegetation coverage.

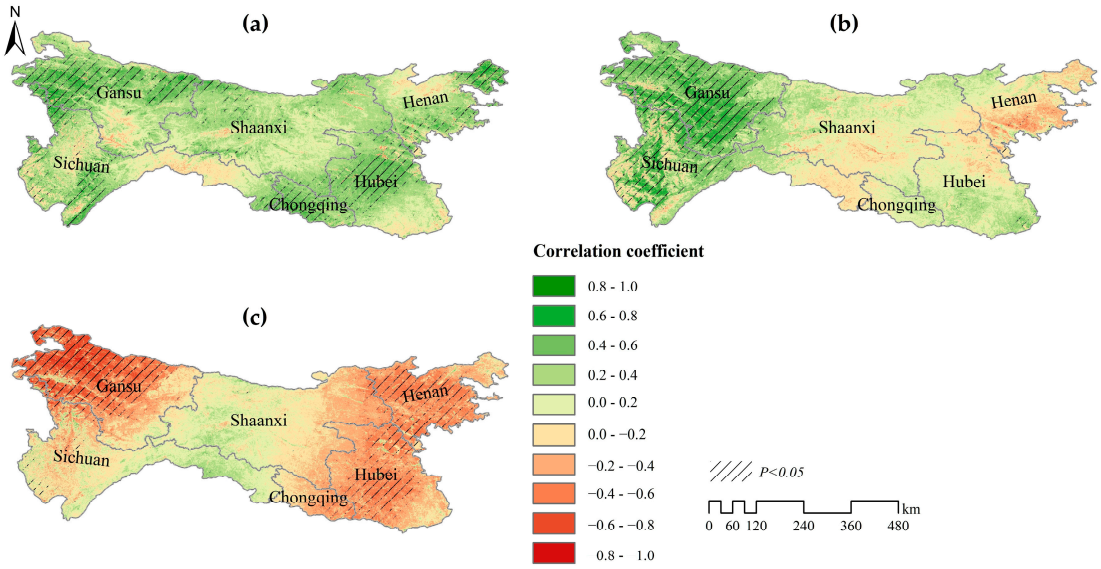

Figure 12. Spatial distribution of the correlation between annual *FVC* and climatic factors in the QBM from 2000–2020: (**a**) *TEM*; (**b**) *PRE*; (**c**) *SSD*.

Table 10. Area proportion of correlation level between *FVC* and climate factors/%.

	1	2	3	4	5
	Significant Positive Correlation	**No significant Positive Correlation**	**Significant Negative Correlation**	**No significant Negative Correlation**	**No Correlation**
TEM	21.10	68.95	0.20	9.02	0.73
PRE	18.55	55.69	0.27	24.75	0.73
SSD	0.26	25.32	20.57	53.13	0.73

Overall (Figure 12b), the annual average *FVC* was positively correlated with the annual *PRE*, mainly in the western region. The strongest positive correlation was in southern Gansu and western Sichuan. Approximately 26% of the regions have a negative correlation between the two, which was mainly distributed in the eastern region, particularly in Nanyang, Henan. This indicates that in the western region the increase in *PRE* over 21 years has improved regional vegetation coverage, whereas in the east, the reduction in *PRE* has increased vegetation coverage.

In the last 21 years, 73.70% of the region's annual average *FVC* had a significant negative correlation with the annual *SSD* (Figure 12c), which was concentrated in the northwest and east. In contrast, the proportion of positive correlation between them was mainly in the central region, but this correlation is weak. This shows that in the 21 years, the increase in annual *SSD* has played a weak role in promoting the improvement of regional vegetation coverage only in the central region. The reduction in annual *SSD* in other regions has greatly improved regional vegetation coverage.

For more than 80% of the regions, there was a positive correlation between the average *FVC* and the average *TEM* in the same season in spring and autumn (Table 11), mainly in the north and west (Figure 13). The negative correlation was mostly to the east of Ankang, and in autumn was mainly at the edge of the Sichuan Basin and around the mountains in western Henan. In summer and winter, the proportion of *FVC* positively correlated with the seasonal average *TEM* was in the range of 60%–70%, but this correlation was weak. In summer, the positive correlation area was concentrated east of Hanzhong, while the negative correlation area was in the south of Gansu. In winter, the positive correlation region was mainly in the northwest and northeast, while the negative correlation was in the central region. In spring, summer, and autumn, the increase in regional vegetation coverage was promoted by an increase in *TEM* in the concurrent season. A decrease in the average *TEM* in the concurrent season was more conducive to the improvement of

vegetation coverage in only a few areas. In contrast, in winter, although the *TEM* in most areas dropped, vegetation coverage still improved.

Table 11. Area proportion of correlation level between *FVC* and *TEM*/%.

	1	2	3	4	5
	Significant Positive Correlation	**No significant Positive Correlation**	**Significant Negative Correlation**	**No significant Negative Correlation**	**No Correlation**
Spring	17.75	64.88	0.19	15.80	1.38
Summer	1.52	59.48	1.54	37.24	0.22
Autumn	10.88	71.42	0.27	16.97	0.45
Winter	3.66	62.41	0.14	31.50	2.29

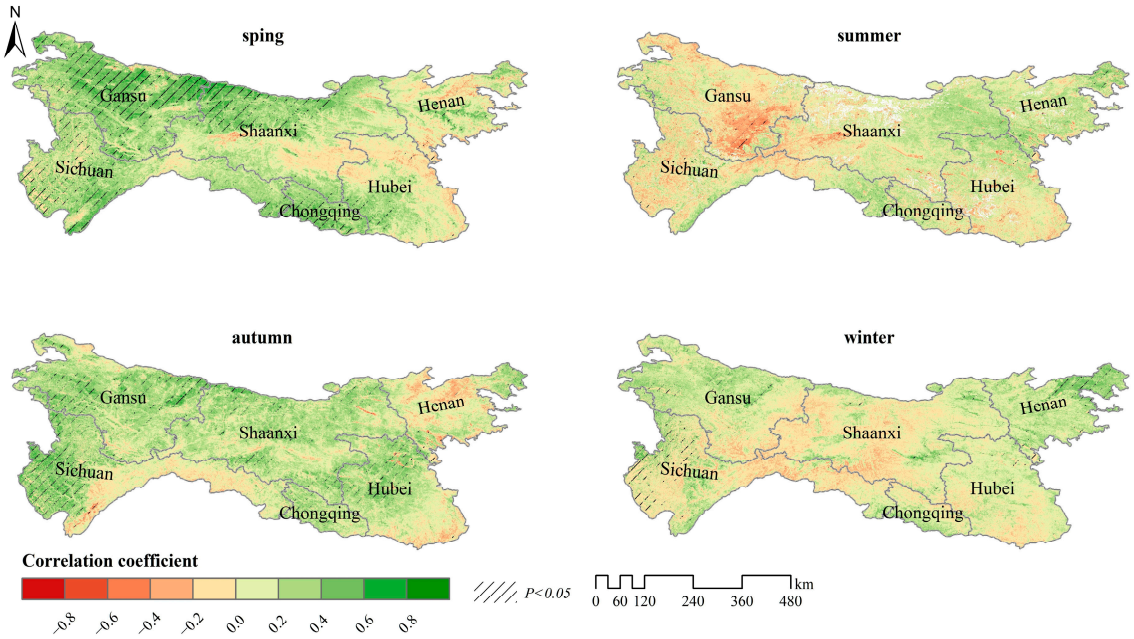

Figure 13. Spatial distribution of the correlation between seasonal *FVC* and *TEM* in the QBM from 2000–2020.

Figure 14 shows that from spring to winter, the proportion of positive correlation area between seasonal average *FVC* and *PRE* in the concurrent season decreased, indicating that the negative correlation between them gradually increased. In spring, regions with a negative correlation accounted for less than 6% (Table 12). In summer and autumn, the proportion of the area with a positive correlation between *FVC* and *PRE* was 55%–68%, but the correlation was slightly weak. In winter, the area of negative correlation was twice that of positive correlation, and it was strong in Tianshui, Baoji, and Mianyang. For the western region, regardless of the season, an increase in *PRE* promoted the improvement of regional vegetation coverage. In most areas, the winter *PRE* decreased, but the vegetation coverage in the current season continued to increase, indicating that the reduction in winter *PRE* may be beneficial to the growth of vegetation.

From the correlation between *FVC* and *SSD* in each season, it was found that the area with negative correlation was largest in autumn, followed by spring and summer, and the area with positive correlation was largest in winter (Table 13). In spring, the negative correlation was mostly in the east, particularly in Henan (Figure 15). The areas with strong negative correlation in summer were concentrated in northwest Gansu. In autumn, the negative correlation area was mainly in the east and west, and the negative correlation was strong. The proportion of the negative correlation area in winter was less than 30%. Although it was distributed in the west and east, it showed a weak negative correlation. Combined with the change trend of seasonal *SSD*, it was found that there was

a decreasing trend in the negative correlation regions, indicating that for most regions, its shortening promotes regional vegetation coverage. However, for the central and Daba Mountain regions, the increase in *SSD* in winter was more beneficial to the increase in vegetation coverage.

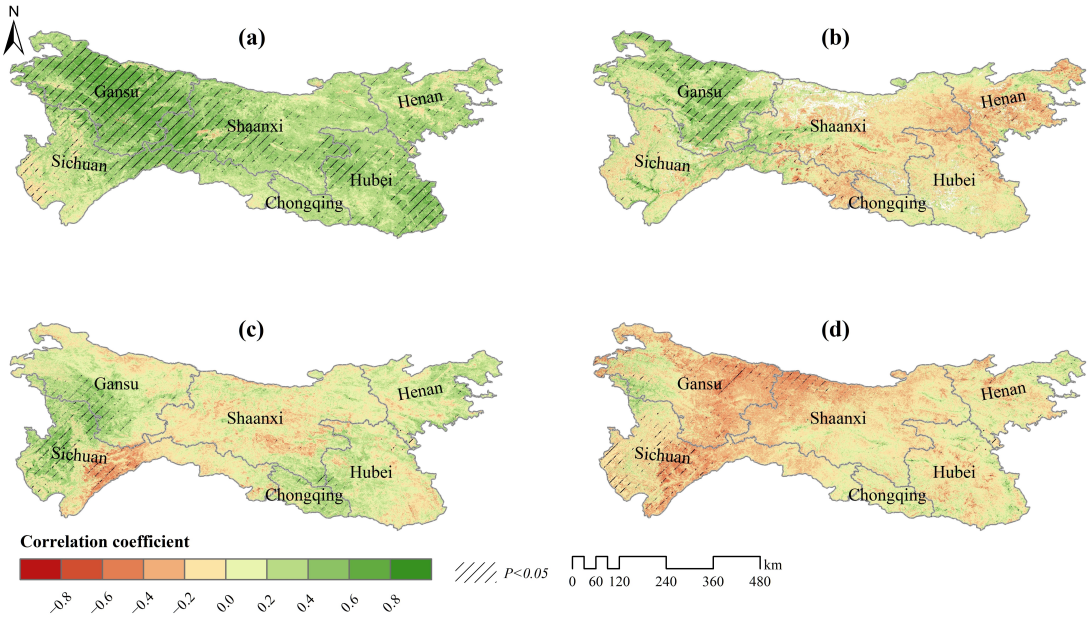

Figure 14. Spatial distribution of the correlation between seasonal *FVC* and *PRE* in the QBM from 2000–2020.

Table 12. Area proportion of correlation level between *FVC* and *PRE*/%.

	1	2	3	4	5
	Significant Positive Correlation	**No significant Positive Correlation**	**Significant Negative Correlation**	**No significant Negative Correlation**	**No Correlation**
Spring	34.84	59.76	0.05	3.96	1.38
Summer	8.84	47.02	2.31	41.61	0.22
Autumn	6.22	60.89	1.13	31.32	0.45
Winter	1.01	32.19	4.62	59.89	2.29

Table 13. Area proportion of correlation level between *FVC* and *SSD*/%.

	1	2	3	4	5
	Significant Positive Correlation	**No significant Positive Correlation**	**Significant Negative Correlation**	**No significant Negative Correlation**	**No Correlation**
Spring	0.45	34.51	7.11	56.54	1.38
Summer	2.70	41.98	7.93	47.15	0.23
Autumn	0.41	17.77	23.69	57.67	0.47
Winter	11.08	62.09	0.39	24.16	2.29

3.3.2. Main Climate Factors of *FVC* Change

From the above analysis, it can be seen that there are obvious differences in the response of *FVC* in different regions to changes in a single climate factor. Therefore, a multiple regression analysis method was adopted to calculate the relative importance of each factor to *FVC* change pixel-by-pixel. In the 21 years in the QBM, the relative importance of the annual average *TEM* (0.33) to *FVC* was greater than that of *PRE* (0.17) and *SSD* (0.20) (Table 14) However, there were clear regional differences in the spatial distribution of the dominant factors. The areas dominated by *TEM* are mainly in the central and eastern regions. The areas mainly controlled by *PRE* change are in western Sichuan, southern Gansu and western Shaanxi, whereas the northwest and east were most affected by *SSD* (Figure 16a).

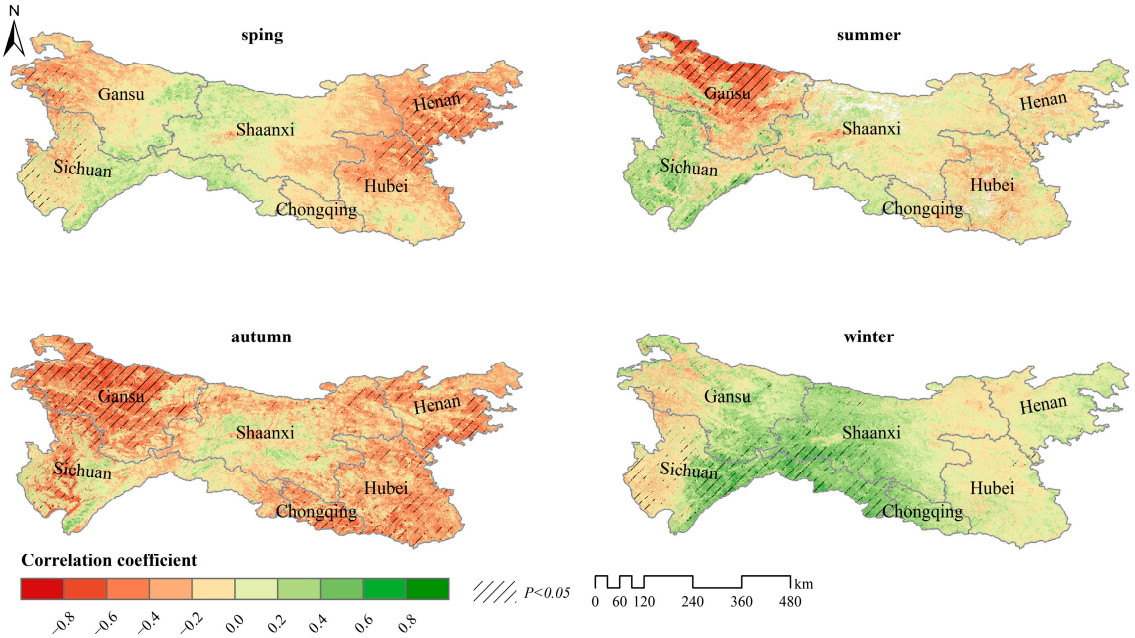

Figure 15. Spatial distribution of the correlation between seasonal *FVC* and *SSD* in the QBM from 2000–2020.

Table 14. Relative importance index of climate factors in the QBM.

		QB	SC	SX	HB	HN	GS	CQ
Year	*TEM*	0.33	0.21	0.30	0.45	0.37	0.36	0.49
	PRE	0.17	0.27	0.17	0.05	−0.01	0.26	0.18
	SSD	−0.20	0.07	−0.05	−0.46	−0.46	−0.31	−0.20
Spring	*TEM*	0.27	0.22	0.24	0.33	0.36	0.27	0.42
	PRE	0.32	0.27	0.38	0.37	0.16	0.40	0.22
	SSD	−0.09	0.06	0.03	−0.22	−0.44	−0.06	−0.16
Summer	*TEM*	0.10	0.00	0.11	0.18	0.29	0.03	0.18
	PRE	0.04	0.08	0.00	−0.06	−0.08	0.20	0.05
	SSD	−0.09	0.15	−0.05	−0.24	−0.28	−0.19	−0.10
Autumn	*TEM*	0.18	0.17	0.23	0.15	0.07	0.20	0.18
	PRE	−0.08	−0.04	−0.14	−0.05	0.02	−0.12	0.07
	SSD	−0.26	−0.13	−0.19	−0.29	−0.28	−0.41	−0.26
Winter	*TEM*	0.06	0.02	−0.01	0.07	0.26	0.06	0.11
	PRE	−0.09	−0.10	−0.12	−0.02	0.03	−0.14	−0.11
	SSD	0.11	0.22	0.19	0.04	−0.04	0.03	0.32

In combination with various regions, Sichuan has the largest relative importance and area proportion of the *PRE* (Figure 17a), mainly in western Sichuan. Although Shaanxi and Chongqing were more affected by *TEM*, Hanzhong was mainly controlled by PRE. In Hubei and Henan, the difference between the relative importance index of *SSD* and the average *TEM* was small, indicating that the regional annual *FVC* change was a result of their joint influence. However, in Shiyan and Zhengzhou, the change in *FVC* was mainly controlled by *TEM*. In contrast to other regions, the relative importance index of the three climate factors in Gansu was basically the same, which indicates that the annual *FVC* changes in this region were affected by the three factors together. The south was mainly controlled by *PRE*, the central and eastern regions are more affected by *TEM*, and the rest are more affected by *SSD*.

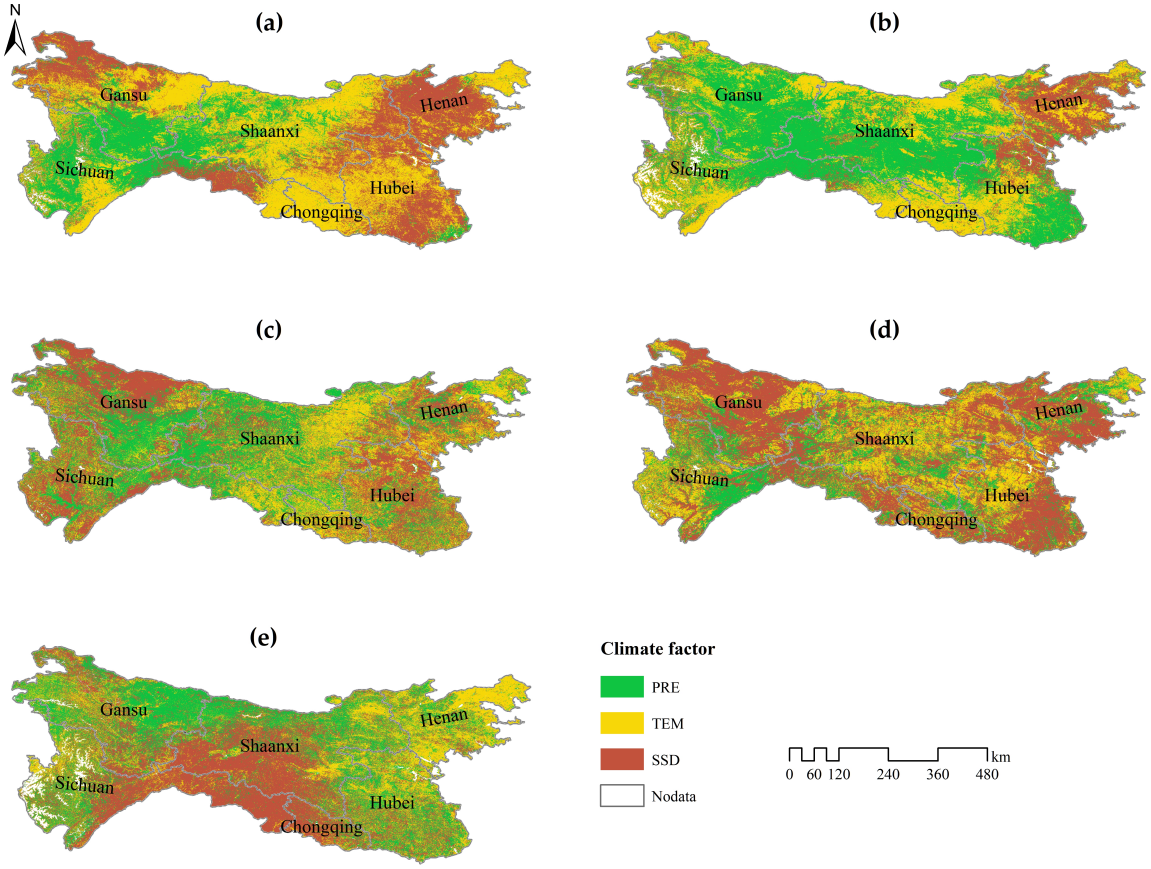

Figure 16. Main climate factors of average *FVC* in the QBM. (**a**) Year; (**b**) Spring; (**c**) Summer; (**d**) Autumn; (**e**) Winter.

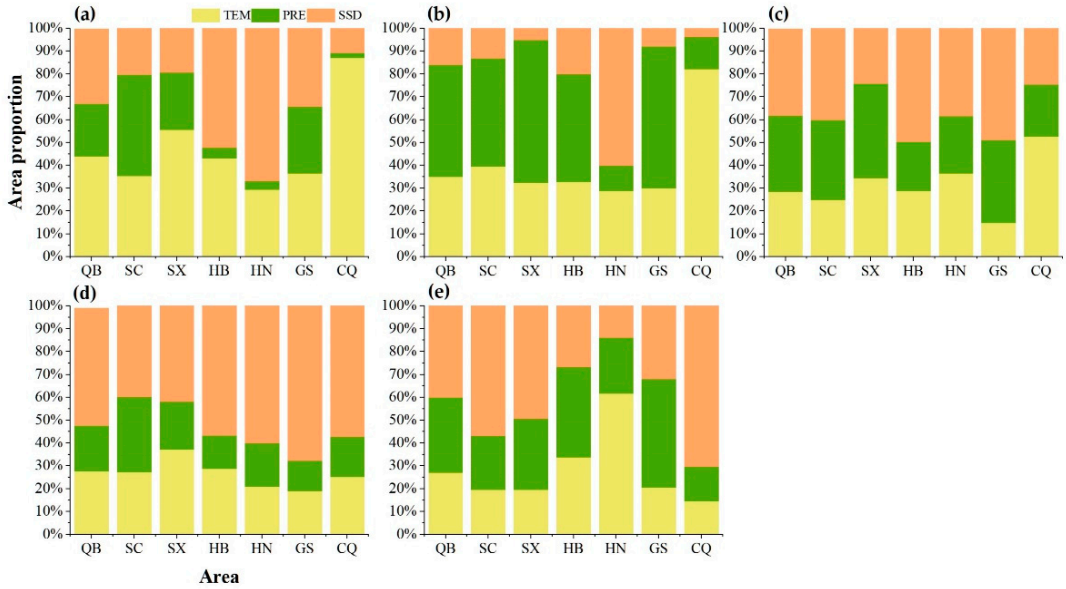

Figure 17. Proportion of the main control area of climate factors in the QBM. (**a**) Year; (**b**) Spring; (**c**) Summer; (**d**) Autumn; (**e**) Winter.

In the past 21 years, the climatic factors leading to *FVC* changes in the QBM have changed significantly during different seasons. In spring, the QBM was more affected by *TEM* and *PRE* (Figure 17b). The former mainly affects the high-altitude areas at the edge, while the latter mainly affects the middle and low-altitude areas in the central and

west (Figure 16b). In summer, although the difference in their relative importance index was small, the area dominated by *SSD* was the largest proportionally (Figure 17c). In autumn, the relative importance of *TEM* and *SSD* was greater. The former was mainly in the east of Shaanxi, whereas the latter is distributed in the east and west (Figure 16d). It was most affected by *SSD* in winter, which was concentrated in the south of Qinling Mountains (Figure 16e).

In addition, the changes in dominant climate factors in different seasons in different regions were also obvious. In spring, Sichuan, Gansu, Shaanxi, and Hubei were affected by *TEM* and PRE. The importance index of *SSD* in Henan was the largest, and the *TEM* in Chongqing was the largest.

In summer, the relative importance of *TEM* and *PRE* weakened, while the influence of *SSD* generally increased. In Sichuan and Gansu, *SSD* and *PRE* had a relatively significant influence on *FVC* changes. Henan and Hubei were affected by *SSD* and *TEM*. Chongqing was mainly affected by *TEM* changes. Although the relative importance of *TEM* in Shaanxi was the largest, the area dominated by *PRE* was larger than that dominated by *TEM*. The change in *FVC* during the summer in this area may be the result of their joint influence.

In autumn, the relative importance of *TEM* and *SSD* on *FVC* changes in most regions increased, *SSD* more than *TEM*, but the impact of *PRE* remained weak. In Sichuan, the relative contribution rate of *TEM* was greater than that of *SSD* and *PRE*, but the areas dominated by the latter two were greater than those of *TEM*, indicating that the region is jointly influenced by the three factors. In Shaanxi, the relative contribution rate of *TEM* was the largest, but the area under the main control of *SSD* was the largest, indicating that the region was jointly affected by *TEM* and *SSD*. In Hubei, Henan, Gansu and Chongqing, the change of *FVC* in autumn in these regions was mainly affected by *SSD*.

In winter, the relative importance of *TEM* decreased, the importance of *PRE* in some areas increased, and *SSD* increased and decreased. In Sichuan and Shaanxi, *FVC* in winter was most influenced by *SSD*, mainly in the north of the Sichuan Basin and Hanshui Valley, whereas other areas were significantly affected by PRE. In Henan, Chongqing, and Gansu, the most important factors were *TEM*, *SSD*, and *PRE*. Although the relative importance of the winter *TEM* in Hubei was the greatest, the main area affected by *PRE* was greater. This shows that the *FVC* changes in winter in this region were the result of the joint action of *TEM* and *PRE*.

4. Discussion

Vegetation activity on a global scale is showing an upward trend [24]. Many studies have shown that in the past 20 years, China's vegetation has been restored, and vegetation coverage has shown a significant increase. However, the average vegetation coverage and its dynamic change trends show obvious spatial heterogeneity. In general, the vegetation coverage in southeast China is higher than that in northwest China. At the same time, the growth trends of the central, eastern, and southwest regions are significant (such as Shaanxi, Gansu, Chongqing, and surrounding regions). This may be related to changes in climate conditions and the adjustment of human activities, such as ecological restoration [25,26]. However, for regions such as the southeast of the Qinghai Tibet Plateau and the northwest Sichuan Plateau, as well as large urban agglomerations with developed economies, because of the terrain, hydrothermal conditions, urban development, and population expansion, the vegetation has showed a significant degradation trend [27–29]. Based on MODWAS *NDVI* data, this study analyzed the dynamic changes in *FVC* in the QBM from 2000–2020. The results showed that vegetation coverage in the QBM was relatively high and showed a significant increasing trend over this period. The regions with rapid growth rates are mainly in the east of Shaanxi, south of Gansu, central Sichuan, and Chongqing. There are a few scattered areas with degraded vegetation in Chengdu and Aba in Sichuan, Hanzhong in Shaanxi, Shiyan in Hubei, Luoyang in Henan, and other urban areas. This result is consistent with the above conclusions.

Changes of climate conditions are widely considered important abiotic factors in the spatial distribution and dynamic change of vegetation [30–32]. In this study, the annual average *TEM* was the main driving factor for changes in vegetation coverage in the QBM. The annual average *FVC* value increased with an increase in annual average *TEM*. There was a positive and negative correlation between annual *PRE* and annual *SSD*,respectively, but these were relatively weak. The area mainly controlled by *TEM* is in the southern foothills of Qinling and Daba Mountains, and the area mainly controlled by *PRE* is in the western high-altitude area. The areas dominated by *SSD* are in the eastern, northwestern, and northern edges of the Sichuan Basin. Previous studies have shown that before reaching a threshold, an increase in *TEM* promotes photosynthesis, prolonging the growth cycle of vegetation, and thus promoting vegetation growth [33,34]. Gao [35] confirmed the reliability of these results. His research results show that in southeast and southwest China, dynamic change in vegetation is most significantly controlled by *TEM*. These areas have abundant rainfall, short *SSD*,and relatively high soil moisture content; therefore, the relationship between vegetation activity and *TEM* was closer. However, for the northern and northwestern regions of China, changes in vegetation cover are most closely related to *PRE* and *SSD* [36–39]. Most of these areas are arid and semi-arid, with long sunshine duration and vegetation growth limited by available moisture. Therefore, an increase in *PRE* and decrease in *SSD* can offset the negative impact of *TEM* rise on vegetation growth, and increase regional vegetation coverage by promoting vegetation growth. However, the results of Kong's study in the Northern Hemisphere for nearly 30 years showed that temperature is a major factor in vegetation greening at high latitudes, especially spring and autumn temperature in North America and Siberia. Solar radiation corresponds well with vegetation trends in northern North America and eastern China [40]. The differences in these results may be related to the differences in the study period and region.

However, under different space-time scales, the main driving factors of changes in vegetation coverage are also different, which is often ignored. Relevant research has shown that dynamic change in vegetation in most regions of China gives the strongest response to spring *TEM*, whereas its positive and negative correlations with *PRE* vary from place to place [41,42]. The present study found that, in the QBM, the positive correlation between changes in vegetation coverage in spring and *PRE* was stronger, the relative impact of the three climate factors was smaller in summer, and the impact of *SSD* was the greatest in autumn and winter. Qi [18] also confirmed the reliability of the results in Qinling area. The results showed that the vegetation growth in the north and south of Qinling Mountains was significantly affected by changes in dry and wet conditions in spring and summer, and that the moisture in spring could promote vegetation growth.

Changes in vegetation coverage are the result of the comprehensive action of climatic and non-climatic factors. In the present study, only climatic factors were considered when focusing on the factors driving changes in vegetation coverage in the QBM. Many other environmental factors also affect the spatial heterogeneity of vegetation dynamic activities, including terrain, soil conditions, and CO_2 concentration. For example, Liu [43] showed that vegetation coverage in the karst region in southwest China is greatly affected by elevation and slope, and vegetation degradation mainly occurs on low-altitude gentle slopes. Shang [44] showed that different soil types could cause differences in vegetation types and attributes. Piao [45] showed that the increase in atmospheric CO_2 concentration and nitrogen deposition are the most likely reasons for the greening trend in China over the past three decades. Therefore, the impact of environmental factors on vegetation should be fully considered in future research.

In addition, on a short time scale, the impact of anthropogenic activities on vegetation growth is very important. In China, the improvement of vegetation coverage in most areas is largely due to the implementation of ecological projects, such as returning farmland to forests/grass, artificial afforestation and grass planting, comprehensive management of rocky desertification [46,47], and appropriate agricultural management measures [48]. However, various human development and utilization activities, such as urban expan-

sion, massive transfer of construction land, illegal logging, and overgrazing have led to the destruction of surface vegetation to a certain extent [49]. This negative impact was particularly evident in large urban agglomerations [24]. Therefore, in subsequent research, it is necessary to quantitatively analyze and evaluate the driving role and mechanism of anthropogenic factors in regional change in vegetation coverage. Furthermore, the separation of the relationship between climatic factors and anthropogenic activity factors will also be the focus of future work.

5. Conclusions

In the present study, we revealed the dynamic change characteristics of vegetation coverage in the QBM of China from 2000–2020 and its response to major climate factors and analyzed the changes in the importance of three climate factors to these changes. The overall distribution of vegetation coverage in the QBM shows a spatial pattern of "low in the east and west and, high in the central." In the past 21 years, regional vegetation coverage has continuously improved, with a faster rising trend in winter and spring. *TEM* showed a spatial distribution pattern that was low in the northwest and high in the southeast, with an obvious warming trend, and warming faster in summer and autumn. The spatial distribution of *PRE* gradually decreased from southeast to northwest. The fluctuation increased in 21 years, with the fastest growth rate occurring in spring. *SSD* generally showed the distribution characteristics of low in the south and high in the north, with a decreasing trend in fluctuation, and the largest decreasing rate in autumn.

The results showed that in the past 21 years, in most areas of the QBM, the change in vegetation coverage was positively correlated with *TEM*, negatively correlated with *SSD*, and both positively and negatively correlated with PRE. On an annual scale, the area mainly affected by *TEM* accounts for approximately 44% of the study area and was mainly in the central and eastern regions. The *SSD* was the main controlling factor affecting the vegetation coverage change in the northwest and east regions. Water condition was the main factor affecting changes in vegetation coverage in western Sichuan, southern Gansu and Hanzhong in Shaanxi. On a seasonal scale, the area dominated by *PRE* in spring was larger. In summer, the relative importance of *TEM* and *PRE* began to weaken, but the area dominated by *SSD* expanded significantly. In autumn, the influence of *TEM* and *SSD* increased, and *SSD* was the main factor affecting vegetation coverage in most areas. Although the relative importance of the three factors was greatly reduced in winter, *SSD* remained the main controlling factor for the change in vegetation coverage in most regions. The research results are helpful in understanding the impact of climate factors on vegetation coverage change in the north-south transitional region of China to better carry out vegetation restoration and protection against the background of global climate change.

Author Contributions: Conceptualization, H.R.; methodology, H.R., C.C. and L.Z. (Lijuan Zhang); software, H.R., Y.L. and L.W.; validation, H.R. and W.Z.; formal analysis, H.R.; investigation, H.R.; resources, H.R.; data curation, H.R.; writing—original draft preparation, H.R.; writing—review and editing, W.Z.; supervision, W.Z.; funding acquisition, L.Z. (Lianqi Zhu). All authors have read and agreed to the published version of the manuscript.

Funding: This research was funded by the National Key Research and Development Program of China, grant number 2021YFE0106700; the National Science and Technology Basic Resource Investigation Program of China, grant number 2017FY100902.

Data Availability Statement: The data presented in this study are available on request from the corresponding author.

Acknowledgments: We thank the School of Geography and Environment, Henan University for providing support.

Conflicts of Interest: The authors declare no conflict of interest.

References

1. Sitch, S.; Smith, B.; Prentice, I.C.; Arneth, A.; Bondeau, A.; Cramer, W.; Kaplan, J.O.; Levis, S.; Lucht, W.; Sykes, M.T.; et al. Evaluation of ecosystem dynamics, plant geography and terrestrial carbon cycling in the LPJ dynamic global vegetation model. *Glob. Chang. Biol.* **2003**, *9*, 161–185. [CrossRef]
2. Sun, R.; Chen, S.; Su, H. Climate Dynamics of the Spatiotemporal Changes of Vegetation NDVI in Northern China from 1982 to 2015. *Remote Sens.* **2021**, *13*, 187. [CrossRef]
3. Myneni, R.B.; Keeling, C.D.; Tucker, C.J.; Asrar, G.; Nemani, R.R. Increased plant growth in the northern high latitudes from 1981 to 1991. *Nature* **1997**, *386*, 698–702. [CrossRef]
4. Tucker, C.J.; Slayback, D.; Pinzon, J.E.; Los, S.; Myneni, R.; Taylor, M.G. Higher northern latitude normalized difference vegetation index and growing season trends from 1982 to 1999. *Int. J. Biometeorol.* **2001**, *45*, 184–190. [CrossRef] [PubMed]
5. Zhang, X. Main Models of Variations of Autumn Vegetation Greenness in the Mid-latitude of North Hemisphere in 1982–2011. *Sci. Geogr. Sin.* **2014**, *34*, 1226–1232. [CrossRef]
6. Myers-Smith, I.H.; Kerby, J.T.; Phoenix, G.K.; Bjerke, J.W.; Epstein, H.E.; Assmann, J.J.; John, C.; Andreu-Hayles, L.; Angers-Blondin, S.; Beck, P.S.A.; et al. Complexity revealed in the greening of the Arctic. *Nat. Clim. Chang.* **2020**, *10*, 106–117. [CrossRef]
7. Jiao, K.; Gao, J.; Wu, S. Climatic determinants impacting the distribution of greenness in China: Regional differentiation and spatial variability. *Int. J. Biometeorol.* **2019**, *63*, 523–533. [CrossRef]
8. Piao, S.; Nan, H.; Huntingford, C.; Ciais, P.; Friedlingstein, P.; Sitch, S.; Peng, S.; Ahlström, A.; Canadell, J.G.; Cong, N.; et al. Evidence for a weakening relationship between interannual temperature variability and northern vegetation activity. *Nat. Commun.* **2014**, *5*, 5018. [CrossRef]
9. Liu, Y.; Li, Y.; Li, S.; Motesharrei, S. Spatial and Temporal Patterns of Global NDVI Trends: Correlations with Climate and Human Factors. *Remote Sens.* **2015**, *7*, 13233–13250. [CrossRef]
10. Zuo, Y.; Li, Y.; He, K.; Wen, Y. Temporal and spatial variation characteristics of vegetation coverage and quantitative analysis of its potential driving forces in the Qilian Mountains, China, 2000–2020. *Ecol. Indic.* **2022**, *143*, 109429. [CrossRef]
11. Wang, S.-H.; Sun, W.; Li, S.-W.; Shen, Z.-X.; Fu, G. Interannual Variation of the Growing Season Maximum Normalized Difference Vegetation Index, MNDVI, and Its Relationship with Climatic Factors on the Tibetan Plateau. *Pol. J. Ecol.* **2015**, *63*, 424–439. [CrossRef]
12. Cui, X.; Bai, H.; Shang, X. The vegetation dynamic in Qinling area based on MODWAS NDVI. *J. Northwest Univ.* **2012**, *42*, 1021–1026. [CrossRef]
13. Guan, L.; Wang, H.; Wang, Y. Dynamic Change of Vegetation Coverage in Sichuan Region Based on GIMMS AVHRR NDVI. *Bullentin Sci. Technol.* **2016**, *32*, 31–36+41. [CrossRef]
14. Zhu, X.; Liu, K.; Li, J.; Zhu, J. Analyswas on Vegetation-Environment Gradient Correlation in Qinling Mountain Based on GWAS. *Res. Soil Water Conserv.* **2009**, *16*, 169–175.
15. Zhang, S.; Bai, H.; Gao, X.; He, Y.; Ren, Y. Spatial-temporal Changes of Vegetation Index and Its Responses to Regional Temperature in Taibai Mountain. *J. Nat. Resour.* **2011**, *26*, 1377–1386. [CrossRef]
16. Ren, Y.; Zhang, Z.; Hou, Q.; He, Y.; Yuan, B. Response of Vegetation Cover Changes to Climate Change in Daba Maintains. *Bullentin Sci. Technol.* **2012**, *2*, 56–59. [CrossRef]
17. Chen, X.; Jiang, H. Climate response of NDVI index on Qinling Mountains in 25 years. *Bull. Surv. Mapp.* **2019**, *3*, 103–107. [CrossRef]
18. Qi, G.; Bai, H.; Zhao, T.; Meng, Q.; Zhang, S. Sensitivity and areal differentiation of vegetation responses to hydrothermal dynamics on the southern and northern slopes of the Qinling Mountains in Shaanxi province. *Acta Geogr. Sin.* **2021**, *76*, 44–56. [CrossRef]
19. Zhang, B. Ten major scientific issues concerning the study of China's north-south transitional zone. *Prog. Geogr.* **2019**, *38*, 305–311. [CrossRef]
20. Long, S.; Guo, Z.; Xu, L.; Zhou, H.; Fang, W.; Xu, Y. Spatiotemporal Variations of Fractional Vegetation Coverage in China based on Google Earth Engine. *Remote Sens. Technol. Appl.* **2020**, *35*, 326–334. [CrossRef]
21. Zhang, X.; Zhu, W.; Cui, Y.; Zhang, J.J.; Zhu, L.Q. The response of forest dynamics to hydro-thermal change in Funiu Mountain. *Geogr. Res.* **2016**, *35*, 1029–1040. [CrossRef]
22. Wang, X.; Hou, X. Variation of Normalized Difference Vegetation Index and its response to extreme climate in coastal China during 1982–2014. *Geogr. Res.* **2019**, *38*, 807–821. [CrossRef]
23. Wang, J.; Wang, K.; Zhang, M.; Zhang, C. Impacts of climate change and human activities on vegetation cover in hilly southern China. *Ecol. Eng.* **2015**, *81*, 451–461. [CrossRef]
24. Eastman, J.R.; Sangermano, F.; Machado, E.A.; Rogan, J.; Anyamba, A. Global Trends in Seasonality of Normalized Difference Vegetation Index (NDVI), 1982–2011. *Remote. Sens.* **2013**, *5*, 4799–4818. [CrossRef]
25. Jin, K.; Wang, F.; Han, Q.; Shi, S.; Ding, W. Contribution of climatic change and human activities to vegetation NDVI change over China during 1982-2015. *Acta Geogr. Sin.* **2020**, *75*, 961–974. [CrossRef]
26. Luo, S.; Liu, Y.; Long, H. Nonlinear trends and spatial pattern analysis of vegetation cover change in China from 1982 to 2018. *Acta Ecol. Sin.* **2022**, *42*, 8331–8342. [CrossRef]

27. Liu, X.; Zhu, X.; Pan, Y.; Li, Y.; Zhao, A. Spatiotemporal changes in vegetation coverage in China during 1982–2012. *Acta Ecol. Sin.* **2015**, *35*, 5331–5342. [CrossRef]
28. Peng, W.; Zhang, D.; Luo, Y.; Tao, S.; Xu, X. Influence of natural factors on vegetation NDVI using geographical detection in Sichuan Province. *Acta Geogr. Sin.* **2019**, *74*, 1758–1776. [CrossRef]
29. Li, H.; Zhang, C.G.; Wang, S.Z.; Ma, W.D.; Liu, F.G.; Chen, Q.; Zhou, Q.; Xia, X.S.; Niu, B.C. Response of vegetation dynamics to hydrothermal conditions on the Qinghai-Tibet Plateau in the last 40 years. *Acta Ecol. Sin.* **2022**, *42*, 4770–4783. [CrossRef]
30. Chen, X.; Wang, H. Spatial and Temporal Variations of Vegetation Belts and Vegetation Cover Degrees in Inner Mongolia from 1982 to 2003. *Acta Geogr. Sin.* **2009**, *64*, 84–94. [CrossRef]
31. Zhu, Z.; Piao, S.; Myneni, R.B.; Huang, M.; Zeng, Z.; Canadell, J.G.; Ciais, P.; Sitch, S.; Friedlingstein, P.; Arneth, A.; et al. Greening of the Earth and its drivers. *Nat. Clim. Chang.* **2016**, *6*, 791–795. [CrossRef]
32. Prăvălie, R.; Sîrodoev, I.; Nita, I.-A.; Patriche, C.; Dumitraşcu, M.; Roşca, B.; Tişcovschi, A.; Bandoc, G.; Săvulescu, I.; Mănoiu, V.; et al. NDVI-based ecological dynamics of forest vegetation and its relationship to climate change in Romania during 1987–2018. *Ecol. Indic.* **2022**, *136*, 108629. [CrossRef]
33. Li, J.; Liu, H.; Li, C.; Li, L. Changes of Green-up Day of Vegetation Growing Season Based on GIMMS 3g NDVI in Northern China in Recent 30 Years. *Sci. Geogr. Sin.* **2017**, *37*, 620–629. [CrossRef]
34. He, Y.; Liu, X.; Wang, H. Variation characteristics of vegetation cover in the latest 10 years over China based on EVI. *J. Meteorol. Sci.* **2017**, *37*, 51–59. [CrossRef]
35. Gao, J.; Jiao, K.; Wu, S. Revealing the climatic impacts on spatial heterogeneity of NDVI in China during 1982–2013. *Acta Geogr. Sin.* **2019**, *74*, 534–543. [CrossRef]
36. Lu, C.; Hou, M.; Liu, Z.; Li, H.; Lu, C. Variation Characterwastic of NDVI and its Response to Climate Change in the Middle and Upper Reaches of Yellow River Basin, China. *IEEE J. Sel. Top. Appl. Earth Obs. Remote Sens.* **2021**, *14*, 8484–8496. [CrossRef]
37. Wu, Z.; Bi, J.; Gao, Y. Drivers and Environmental Impacts of Vegetation Greening in a Semi-Arid Region of Northwest China since 2000. *Remote Sens.* **2021**, *13*, 4246. [CrossRef]
38. Zou, Y.; Chen, W.; Li, S.; Wang, T.; Yu, L.; Xu, M.; Singh, R.P.; Liu, C.-Q. Spatio-Temporal Changes in Vegetation in the Last Two Decades (2001–2020) in the Beijing–Tianjin–Hebei Region. *Remote Sens.* **2022**, *14*, 3958. [CrossRef]
39. Cao, W.; Xu, H.; Zhang, Z. Vegetation Growth Dynamic and Sensitivity to Changing Climate in a Watershed in Northern China. *Remote Sens.* **2022**, *14*, 4198. [CrossRef]
40. Kong, D.; Zhang, Q.; Singh, V.P.; Shi, P. Seasonal vegetation response to climate change in the Northern Hemisphere (1982–2013). *Glob. Planet. Chang.* **2016**, *148*, 1–8. [CrossRef]
41. Zhang, X.; Dai, J.; Ge, Q. Spatial Differences of Changes in Spring Vegetation activities across Eastern China during 1982–2006. *Acta Geogr. Sin.* **2012**, *67*, 53–61. [CrossRef]
42. Wang, Y.; Wang, Y.; Wang, J.; Li, W. Transient and Lagged Response of Seasonal Vegetation Changes to Climate in China during the Past Two Decades. *Geogr. Geo-Inf. Sci.* **2020**, *4*, 33–40. [CrossRef]
43. Liu, L.; Zhan, C.; Hu, S.; Dong, Y. Vegetation change and its topographic effects in the karst mountainous areas of Guizhou and Guangxi. *Geogr. Res.* **2018**, *37*, 2433–2446. [CrossRef]
44. Shang, B.; Zheng, B.; Zhou, Z.; Wang, Z.; Wang, L. Vegetation Growth and Its Influencing Factors under Different Soil Conditions in Mayi Lake Area of Kelamayi City. *J. Northeast. For. Univ.* **2021**, *1*, 44–49. [CrossRef]
45. Piao, S.; Yin, G.; Tan, J.; Cheng, L.; Huang, M.; Li, Y.; Liu, R.; Mao, J.; Myneni, R.B.; Peng, S.; et al. Detection and attribution of vegetation greening trend in China over the last 30 years. *Glob. Chang. Biol.* **2015**, *21*, 1601–1609. [CrossRef] [PubMed]
46. LV, Y.; Zhang, L.; Yan, H.; Ren, X.; Wang, J.; Niu, Z.; Gu, X.; He, H. Spatial and temporal patterns of changing vegetation and the influence of environmental factors in the karst region of Southwest China. *Acta Ecol. Sin.* **2018**, *38*, 8774–8786. [CrossRef]
47. Zhao, Z.; Han, R.; Guan, X.; Xiao, W.; Li, J. Change of vegetation coverage and the driving factor in the Beijing-Tianjin-Hebei region from 2000 to 2019. *Acta Ecol. Sin.* **2022**, *42*, 8860–8868. [CrossRef]
48. Zhang, L.; Liang, C.; Ma, H.; Chen, X.; Cai, J.; Guo, R.; Chen, T. The potential contribution of land managements to vegetation greening: A case study of the northeast agricultural region in China. *Acta Ecol. Sin.* **2022**, *42*, 720–731. [CrossRef]
49. Sun, Y.; Yi, L.; Yin, S. Vegetation Cover Change in Dongting Lake Basin and Its Coordination Governance. *Econ. Geogr.* **2022**, *4*, 190–201. [CrossRef]